

## Article

# Synthesis and Characterization of New Pyrano[2,3-*c*]pyrazole Derivatives as 3-Hydroxyflavone Analogues

 Arminas Urbonavičius<sup>1,2</sup>, Sonata Krikštolaitytė<sup>1</sup>, Aurimas Bieliauskas<sup>2</sup> , Vytas Martynaitis<sup>1</sup> ,  
 Joana Solovjova<sup>1</sup>, Asta Žukauskaitė<sup>1,3</sup> , Eglė Arbačiauskienė<sup>1,\*</sup>  and Algirdas Šačkus<sup>2,\*</sup>

<sup>1</sup> Department of Organic Chemistry, Kaunas University of Technology, Radvilėnų pl. 19, LT-50254 Kaunas, Lithuania; arminas.urbonavicius@ktu.lt (A.U.); sonata.krikstolaityte@ktu.lt (S.K.); vytas.martynaitis@ktu.lt (V.M.); joana.solovjova@ktu.lt (J.S.); asta.zukauskaite@upol.cz (A.Ž.)

<sup>2</sup> Institute of Synthetic Chemistry, Kaunas University of Technology, K. Baršausko g. 59, LT-51423 Kaunas, Lithuania; aurimas.bieliauskas@ktu.lt

<sup>3</sup> Department of Chemical Biology, Palacký University, Šlechtitelů 27, CZ-78371 Olomouc, Czech Republic

\* Correspondence: egle.arbaciauskiene@ktu.lt (E.A.); algirdas.sackus@ktu.lt (A.Š.)

**Abstract:** In this paper, an efficient synthetic route from pyrazole-chalcones to novel 6-aryl-5-hydroxy-2-phenylpyrano[2,3-*c*]pyrazol-4(2*H*)-ones as 3-hydroxyflavone analogues is described. The methylation of 5-hydroxy-2,6-phenylpyrano[2,3-*c*]pyrazol-4(2*H*)-one with methyl iodide in the presence of a base yielded a compound containing a 5-methoxy group, while the analogous reaction of 5-hydroxy-2-phenyl-6-(pyridin-4-yl)pyrano[2,3-*c*]pyrazol-4(2*H*)-one led to the zwitterionic 6-(*N*-methylpyridinium)pyrano[2,3-*c*]pyrazol derivative. The treatment of 5-hydroxy-2,6-phenylpyrano[2,3-*c*]pyrazol-4(2*H*)-one with triflic anhydride afforded a 5-trifloylsubstituted compound, which was further used in carbon–carbon bond forming Pd-catalyzed coupling reactions to yield 5-(hetero)aryl- and 5-carbo-functionalized pyrano[2,3-*c*]pyrazoles. The excited-state intramolecular proton transfer (ESIPT) reaction of 5-hydroxypyano[2,3-*c*]pyrazoles from the 5-hydroxy moiety to the carbonyl group in polar protic, polar aprotic, and nonpolar solvents was observed, resulting in well-resolved two-band fluorescence. The structures of the novel heterocyclic compounds were confirmed by <sup>1</sup>H-, <sup>13</sup>C-, <sup>15</sup>N-, and <sup>19</sup>F-NMR spectroscopy, HRMS, and single-crystal X-ray diffraction data.

**Keywords:** pyrazoles; pyrano[2,3-*c*]pyrazoles; 3-hydroxyflavone; Algar–Flynn–Oyamada reaction; NMR investigation; ESIPT



**Citation:** Urbonavičius, A.; Krikštolaitytė, S.; Bieliauskas, A.; Martynaitis, V.; Solovjova, J.; Žukauskaitė, A.; Arbačiauskienė, E.; Šačkus, A. Synthesis and Characterization of New Pyrano[2,3-*c*]pyrazole Derivatives as 3-Hydroxyflavone Analogues. *Molecules* **2023**, *28*, 6599. <https://doi.org/10.3390/molecules28186599>

Academic Editors: Vera L. M. Silva and Artur M. S. Silva

Received: 12 July 2023

Revised: 1 September 2023

Accepted: 9 September 2023

Published: 13 September 2023



**Copyright:** © 2023 by the authors. Licensee MDPI, Basel, Switzerland. This article is an open access article distributed under the terms and conditions of the Creative Commons Attribution (CC BY) license (<https://creativecommons.org/licenses/by/4.0/>).

## 1. Introduction

Fused pyrazole derivatives represent an important class of organic compounds as they are found in a large number of biologically and chemically active compounds [1]. These compounds are known for their anticancer [2], antimicrobial [3], antiviral [4], and anti-coagulant properties [5], and for their activity against CNS disorders [6]. Some of the fused pyrazole moieties are present in marketed drugs, such as apixaban, sildenafil, indiplon, zaleplon, etazolate, cartazolate, allopurinol, and futibatinib, which was recently approved by the U.S. Food and Drug Administration (FDA) [7].

Among other fused systems, pyrano[2,3-*c*]pyrazoles have been investigated for analgesic and anti-inflammatory [8], antimicrobial [9,10], and anticancer [11] activities. Recently, Sun et al. described the nano-formulation and anticancer activity of a 6-amino-4-(2-hydroxyphenyl)-3-methyl-1,4-dihydropyrano[2,3-*c*]pyrazole-5-carbonitrile via the blocking of the cell cycle through a p53-independent pathway [12], while Nguyen et al. reported a four-component sulfonated amorphous carbon and eosin Y-catalyzed synthesis and the molecular docking of 6-amino-1,4- or 2,4-dihydropyrano[2,3-*c*]pyrazole-5-carbonitriles as inhibitors of p38 MAP kinase [13]. In our previous studies, we reported the synthesis, characterization, and biological evaluation of several pyrano[2,3-*c*]pyrazole derivatives [14,15].

However, 5-hydroxy-2,6-diarylpyrano[2,3-*c*]pyrazol-4(2*H*)-ones, which can serve as potential analogues of 3-hydroxyflavone, are still understudied.

3-Hydroxyflavone **I** (Figure 1) is known as the backbone of all flavonols. Flavonols are a class of the flavonoid family, a group of naturally occurring substances with variable phenolic structures, found in fruits, vegetables, grains, bark, roots, stems, flowers, tea, and wine [16–18]. Quercetin **II** and kaempferol **III** (Figure 1) are the most prevalent in plants and are among the flavonols that have been most investigated and reviewed for beneficial health properties, such as antioxidant, antimicrobial, hepatoprotective, and anti-inflammatory properties, and other effects [19,20]. Synthetic and semisynthetic flavonol derivatives have been reported in the literature in an attempt to improve the biochemical and pharmacological properties of their corresponding natural compounds. For example, synthesis and anti-*Leishmania* activity were reported for benzothiophene-flavonols [21]. A series of spirochromone-flavonols [22] and thiophene-pyrazole-flavonols [23] was synthesized and tested as antimicrobial agents. In addition, flavonols containing an isothiazolidine ring have been found to be effective inhibitors of cyclin-dependent kinase 2 (CDK2) [24].

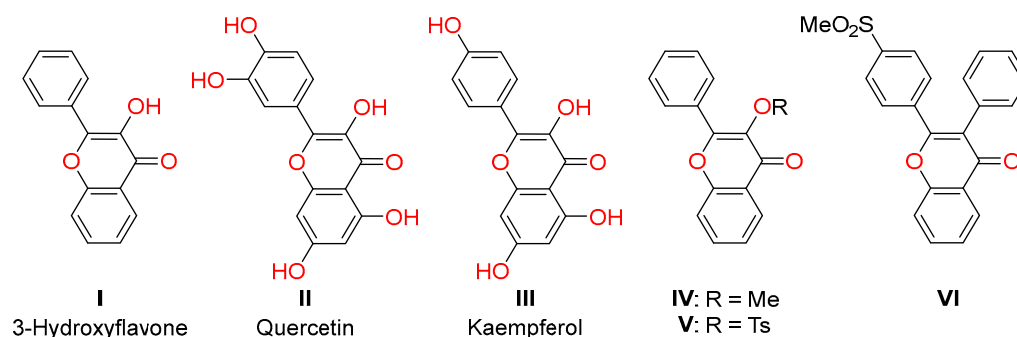


**Figure 1.** Structural formulas of selected 3-hydroxyflavones and their relative compounds.

3-Hydroxyflavones are known as fluorescent dyes because of their typical excited-state intramolecular photon transfer (ESIPT). ESIPT is one type of proton transfer reaction that has been the subject of considerable interest and a number of investigations in recent decades [25,26]. 3-Hydroxyflavones have been investigated as therapeutic imaging agents, including as fluorescence sensors and probes for the detection of the microenvironment, metal ions, and structures of proteins and DNA [27–30]. For example, Jiang et al. reported the application of 3-hydroxyflavone-based ESIPT fluorescent dyes for the dynamic imaging of lipid droplets with cells and tissues [31]. In a study by Kamariza et al., a 3-hydroxychromone derivative, 2-[7-(diethylamino)-9,9-dimethyl-9*H*-fluoren-2-yl]-3-hydroxy-4*H*-chromen-4-one, was conjugated to trehalose and a bright solvatochromic dye was obtained that detects *Mycobacterium tuberculosis* in a matter of minutes [32].

The *O*-methylation of 3-hydroxyflavones with reagents such as diazomethane, methyl iodide, dimethyl sulfate, or dimethyl carbonate proceeded to give *O*-methylated flavonoids, which exhibited a variety of biological activities [33–35]. For example, Ohtani et al. investigated the effect of 3-methoxyflavone derivatives, such as those of compound **IV** (Figure 1), on *P*-glycoprotein by measuring the potentiation of cellular accumulation and growth inhibition [36]. Juvale et al. reported the inhibitory activity of 3-methoxyflavones against a breast cancer resistance protein (BVRP/ABCG2) [37]. Furthermore, 3-hydroxyflavone treated with *p*-TsCl in the presence of a base afforded a corresponding flavone tosylate **V**, which was used in a Suzuki–Miyaura reaction for cross coupling with various phenyl boronic acids to give 2,3-diarylbenzopyrans [38,39]. Flavone-like 2,3-diarylbenzopyrans, such as compound **VI** (Figure 1), have been synthesized as novel selective inhibitors of cyclooxygenase-2 [40,41].

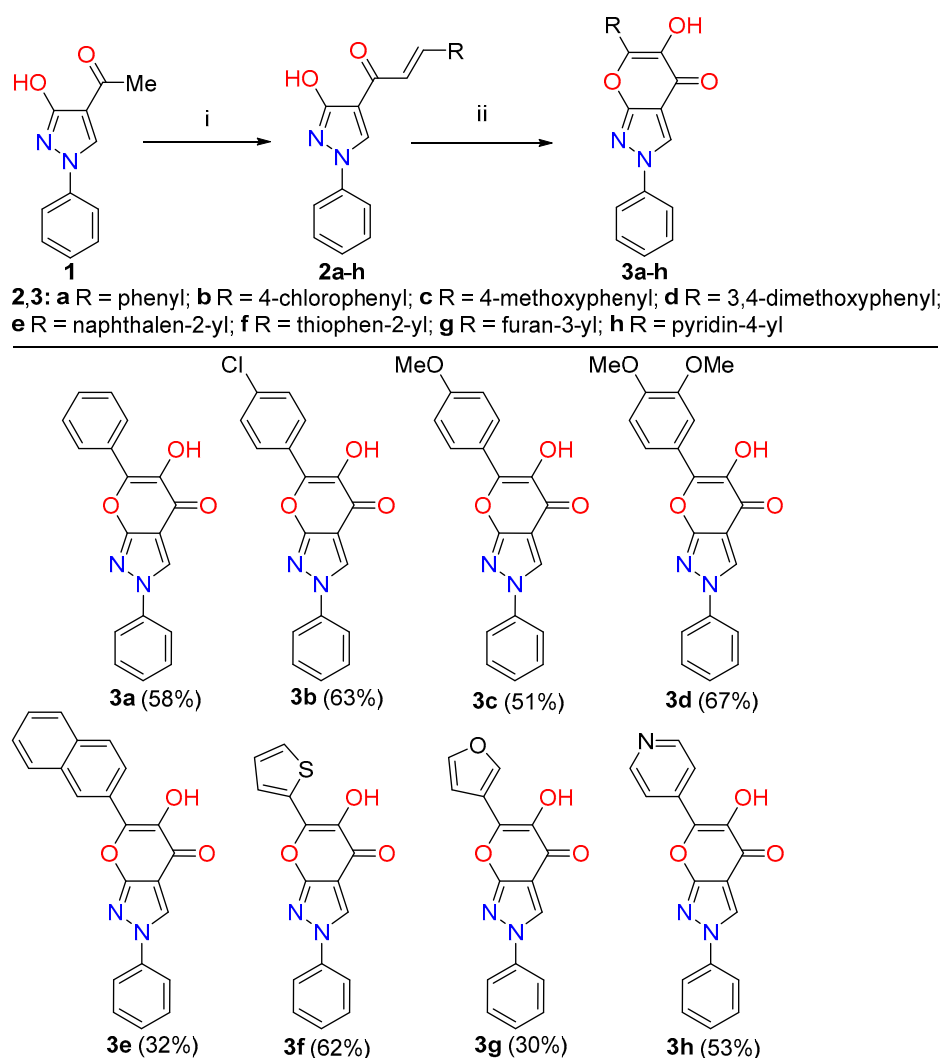
In the continuation of our research on the development of novel fused heterocyclic pyrazole-containing systems, we report here the synthesis, structural elucidation, and optical properties of novel 6-aryl-5-hydroxy-2-phenylpyrano[2,3-*c*]pyrazol-4(2*H*)-one deriva-

tives as analogues of 3-hydroxyflavones. The ESIPT reaction of 6-aryl-5-hydroxy-2-phenylpyrano[2,3-*c*]pyrazol-4(2*H*)-ones from the 5-hydroxy moiety to the carbonyl group in MeOH and polar aprotic and non-polar solvents was also investigated. The obtained 5-hydroxy-2-phenylpyrano[2,3-*c*]pyrazol-4(2*H*)-ones were further functionalized by methylation as well as the Pd-catalyzed Suzuki, Heck, and Sonogashira coupling reactions of intermediate 5-triflate.

## 2. Results and Discussion

### 2.1. Chemistry

The synthesis of 6-(hetero)aryl-5-hydroxy-2-phenylpyrano[2,3-*c*]pyrazol-4(2*H*)-ones **3a–h** was carried out as depicted in Scheme 1. 1-Phenyl-1*H*-pyrazol-3-ol **1** was obtained using a previously reported method [42,43] and subjected to a Claisen–Schmidt condensation reaction with variously 4'-substituted (hetero)aryl aldehydes in the presence of ethanolic sodium hydroxide, as we have described [44]. Heating the reaction mixture at 55 °C for 3 to 5 h afforded (*E*)-1-(3-hydroxy-1-phenyl-1*H*-pyrazol-4-yl)prop-2-en-1-ones **2a–h** in poor to excellent yields (36–95%).



**Scheme 1.** Reagents and conditions: (i) appropriate carbaldehyde, NaOH, EtOH, 55 °C, 3–5 h, in accordance with ref. [44]; (ii) NaOH, EtOH, H<sub>2</sub>O<sub>2</sub>, –25 °C, 2 h, then rt, 16 h.

In a subsequent step, an Algar–Flynn–Oyamada (AFO) synthetic approach was applied for the formation of novel pyrano[2,3-*c*]pyrazol-4(2*H*)-ones **3a–h**. The AFO reaction is a stepwise process whereby chalcones undergo an oxidative cyclization to form flavones in

the presence of alkaline hydrogen peroxide [45]. The AFO reaction outcome is dependent on the choice of the base; therefore, chalcone **2a** was used as a model compound for the fine-tuning of the reaction conditions. Several organic and inorganic bases (NaOH, KOH, NaOAc, TEA, and NaHCO<sub>3</sub>) were screened in different mixtures of ethanol/water as a solvent and a divergent amount of hydrogen peroxide (Table S1). The best result was obtained when using NaOH in EtOH and employing 5 eq of H<sub>2</sub>O<sub>2</sub>. Stirring chalcones **2a–h** with hydrogen peroxide in an alkaline ethanolic solution at  $-25\text{ }^{\circ}\text{C}$  for 2 h and at room temperature overnight afforded the flavanol analogues **3a–h** in poor to good yields (30–67%). The pyrano[2,3-*c*]pyrazol-4(2*H*)-ones **3e** and **3g** were obtained in lower yields (30–32%) when chalcones bearing naphthalen-2-yl or furan-3-yl substituents (**2e** and **2g**, respectively) were used as starting materials in the AFO reaction. Unfortunately, the AFO reaction of (*E*)-3-(4-fluorophenyl)-1-(3-hydroxy-1-phenyl-1*H*-pyrazol-4-yl)prop-2-en-1-one or its 3-(4-nitrophenyl) counterpart gave only traces of targeted pyrano[2,3-*c*]pyrazol-4(2*H*)-ones.

According to the mechanistic studies reported in the literature [45–47], the formation of 6-(hetero)aryl-5-hydroxy-2-phenylpyrano[2,3-*c*]pyrazol-4(2*H*)-ones **3** from (*E*)-1-(3-hydroxy-1-phenyl-1*H*-pyrazol-4-yl)prop-2-en-1-ones **2**, employing AFO reaction conditions could proceed according to two different pathways, as depicted in Figure 2, using the transformation of **2a** to **3a** as an example. According to the approach suggested by Shen et al., first epoxide **A** (Figure 2, path A) is formed; then it is subsequently cyclized to 5-hydroxy-2,6-diphenyl-5,6-dihydropyrano[2,3-*c*]pyrazol-4(2*H*)-one **B** and oxidized to target 5-hydroxy-2-phenylpyrano[2,3-*c*]pyrazol-4(2*H*)-one **3a** [45]. Alternatively, as suggested by Ferreira et al., pyrazole-chalcone **2a** might first undergo a cyclization forming a 2,6-diphenyl-2,6-dihydropyrano[2,3-*c*]pyrazol-4-olate **C** (Figure 2, path B), followed by an attack of hydrogen peroxide and subsequent oxidation to form **3a** [47].

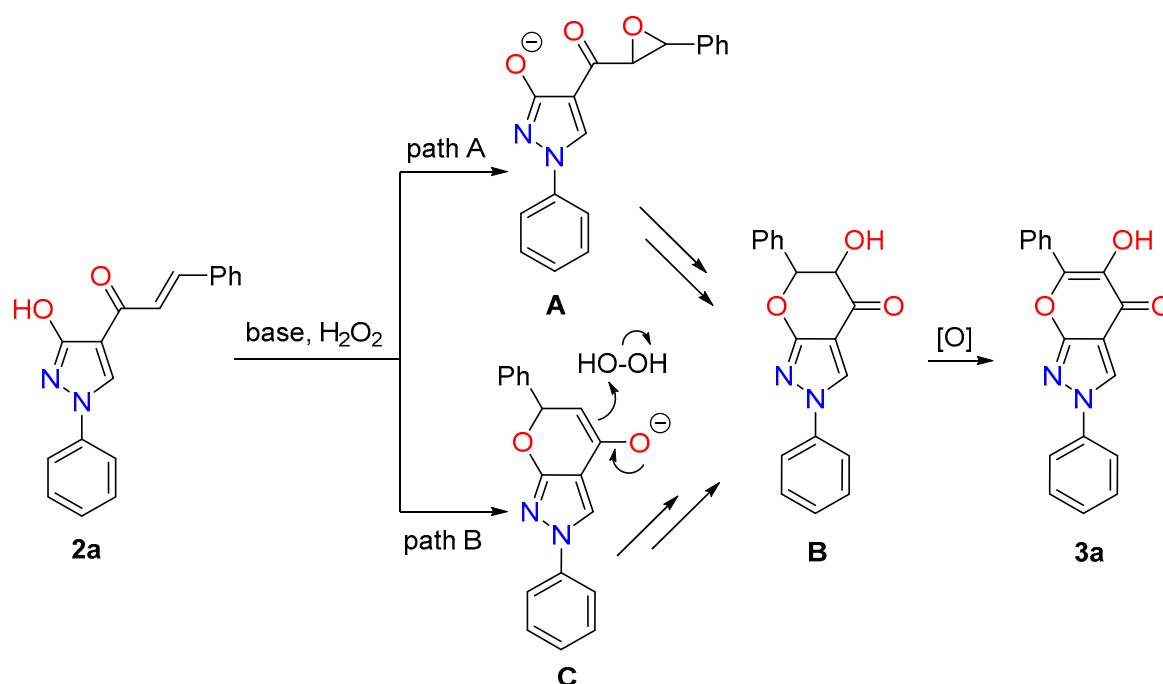
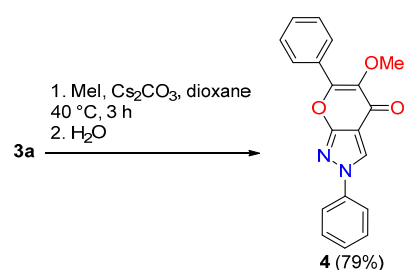


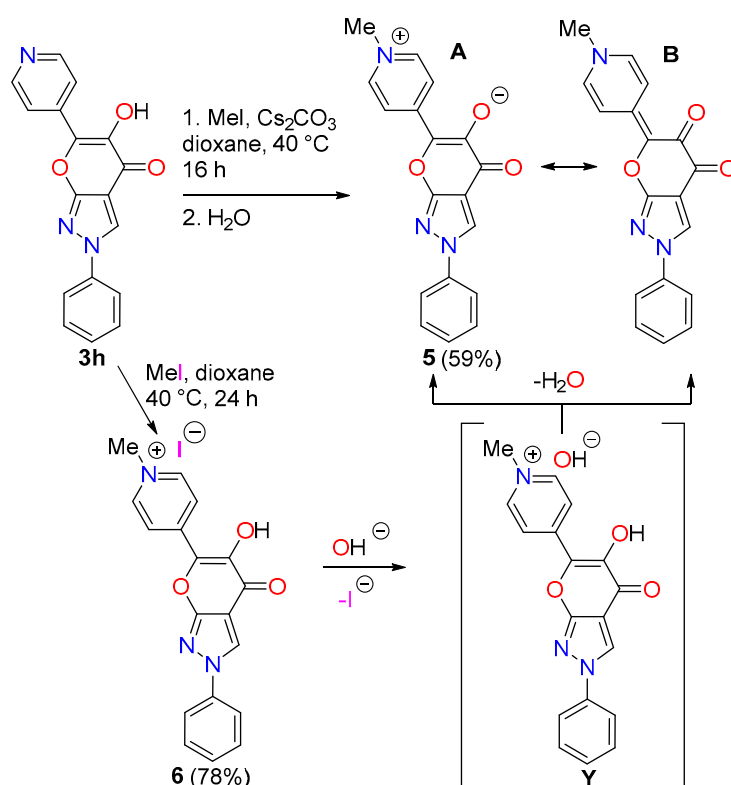
**Figure 2.** Mechanisms proposed for the transformation reaction of compound **2a** to compound **3a**.

For further modification of the obtained flavanol analogue **3a**, *O*-alkylation reaction conditions were applied. As a result, treating **3a** with methyl iodide in the presence of cesium carbonate in dioxane at  $40\text{ }^{\circ}\text{C}$  gave *O*-methylated compound **4** in a 79% yield (Scheme 2).



**Scheme 2.** O-Methylation of compound **3a**.

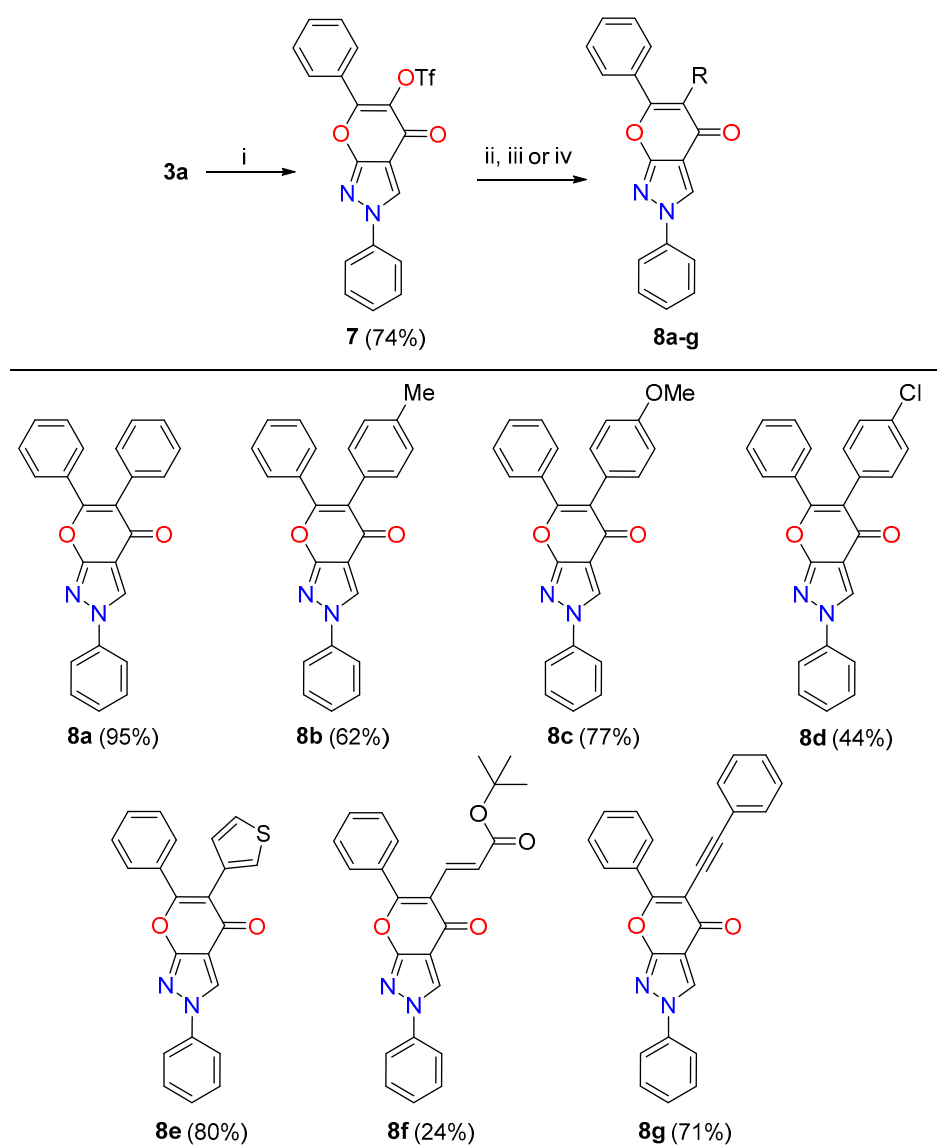
Subsequently the methylation of compound **3h** containing both the hydroxyl group and the pyridin-4-yl substituent was investigated (Scheme 3). With the alkylation reaction conditions described above (MeI, Cs<sub>2</sub>CO<sub>3</sub>, dioxane, 40 °C), a formation of zwitterionic pyrano[2,3-*c*]pyrazol derivative **5** as the main product was observed.



**Scheme 3.** N-Methylation of compound **3h**.

The proposed mechanism for the formation of compound **5** is shown in Scheme 3. Presumably, first, as a result of the reaction of pyridinyl-containing compound **3h** with methyl iodide, methylpyridinium iodide **6** was formed. This was also demonstrated when alkylating compound **3h** in the absence of a base as salt **6** was obtained in a 78% yield. The subsequent treatment of methylpyridinium iodide **6** with a base led to the formation of methylpyridinium hydroxide **Y**, which, upon the removal of the water molecule, led to the formation of the corresponding structure **5** as a resonance hybrid with the two contributing forms **A** and **B**, zwitterionic and neutral molecular structures, respectively. Pat et al. investigated the two-photon absorption (TPA) processes in a class of 4-quinopyran chromophores. The neutral molecular structure with a quinoid geometry is the molecular ground state, while the zwitterionic configuration with a benzenoid structure contributes significantly. The bond connecting the donor and acceptor phenylene fragments is a double bond when the molecule is neutral, while it is a single bond for the zwitterionic structure [48].

Further functionalization of pyrano[2,3-*c*]pyrazol-4(2*H*)-ones was accomplished via *O*-triflate intermediate **7**, which was synthesized from 5-hydroxy-2,6-diphenylpyrano[2,3-*c*]pyrazol-4(2*H*)-one (**3a**) following a standard procedure using  $\text{TiF}_2\text{O}$  in the presence of TEA (Scheme 4). The obtained 4-oxo-2,4-dihydropyrano[2,3-*c*]pyrazol-5-yl trifluoromethanesulfonate **7** was subjected to Suzuki, Heck, and Sonogashira reactions to examine the employment of Pd-catalyzed coupling reactions for the functionalization of pyrano[2,3-*c*]pyrazol-4(2*H*)-ones. Triflate **7** underwent Suzuki-type cross coupling with (hetero)aryl boronic acids to give compounds **8a–e** in fair to excellent yields (44–95%). In the course of this coupling, standard conditions were applied, i.e.,  $\text{Pd}(\text{PPh}_3)_4$  was used as a catalyst and anhydrous  $\text{K}_3\text{PO}_4$  as a base in dioxane at 90 °C. The reaction was carried out in the presence of KBr, which is known to suppress the decomposition of the palladium catalyst transition state by converting phosphonium salts to palladium bromide [49]. The Suzuki reaction yield was lower (44%) when 4-chlorophenylboronic acid was used for the cross coupling.



**Scheme 4.** Reagents and conditions: (i) TEA,  $\text{TiF}_2\text{O}$ , DCM, 0–24 °C, 16 h; (ii) (hetero)aryl boronic acid,  $\text{K}_3\text{PO}_4$ , KBr,  $\text{Pd}(\text{PPh}_3)_4$ , dioxane, 90 °C, 16 h (for **8a–e**); (iii) *tert*-butyl acrylate, TEA,  $\text{Pd}(\text{PPh}_3)_2\text{Cl}_2$ , DMF (dry), 100 °C (for **8f**), 72 h; (iv) phenylacetylene, TEA, CuI,  $\text{Pd}(\text{PPh}_3)_2\text{Cl}_2$ , DMF (dry), 65 °C, 1 h (for **8g**).

The Heck reaction of triflate **7** and *tert*-butyl acrylate under the standard conditions (Pd(PPh<sub>3</sub>)<sub>2</sub>Cl<sub>2</sub>, TEA, DMF, 100 °C) gave a poor yield (24%) of *tert*-butyl (*E*)-3-(4-oxo-2,4-dihydropyrano[2,3-*c*]pyrazol-5-yl)acrylate **8f**, while the Sonogashira cross-coupling reaction of compound **7** with phenylacetylene under the usual conditions (Pd(PPh<sub>3</sub>)<sub>2</sub>Cl<sub>2</sub>, CuI, TEA, DMF, 65 °C) afforded alkyne **8g** in a good yield (71%). A similar approach of flavonol functionalization employing Pd-catalyzed reactions of *O*-triflates was also reported by Kumar et al. in their study on the synthesis of 3,4-diarylpyrazoles and 4,5-diarylpyrimidines, starting with triaryl bismuth as a three-fold arylating reagent and 3-trifloxychromones [50]. Dahlén et al. reported a synthetic strategy to form 2,3,6,8-tetrasubstituted chromone derivatives employing a Stille coupling reaction for the functionalization of the third position of the ring via intermediate 4-oxo-4*H*-chromen-3-yl trifluoromethanesulfonates [51]. Notably, it was observed that the latter compounds were not active under Heck reaction conditions. In addition, Akwari et al. demonstrated effective 3-arylation of flavones via a Suzuki cross-coupling reaction of 3-(trifluorosulphonyloxy)flavone [52].

## 2.2. NMR Spectroscopic Investigations

The formation of 6-(hetero)aryl-5-hydroxy-2-phenylpyrano[2,3-*c*]pyrazol-4(2*H*)-ones **3a–h** and their derivatives **4**, **5**, **6**, **7**, and **8a–g** was confirmed through detailed analysis of their spectroscopic data. Key information for structure elucidation was obtained from NMR spectral data using a combination of standard and advanced NMR spectroscopy techniques, such as <sup>1</sup>H-<sup>13</sup>C HMBC, <sup>1</sup>H-<sup>13</sup>C LR-HSQMBC, <sup>1</sup>H-<sup>15</sup>N HMBC, <sup>1</sup>H-<sup>13</sup>C HSQC, <sup>1</sup>H-<sup>13</sup>C H2BC, <sup>1</sup>H-<sup>1</sup>H COSY, <sup>1</sup>H-<sup>1</sup>H TOCSY, <sup>1</sup>H-<sup>1</sup>H NOESY, and 1,1-ADEQUATE experiments. Since popular NMR prediction programs such as CSEARCH, ACD C+H predictor, as well as NMR chemical shift databases for structural dereplication depend on high-quality data with unambiguously assigned resonances [53], we carried out NMR studies with the obtained compounds to fully map all the <sup>1</sup>H, <sup>13</sup>C and <sup>15</sup>N NMR signals as accurately as possible. The corresponding NMR data for the selected representatives of the aforementioned new ring systems are displayed in Figures 3 and 4.

An initial comparison of the <sup>1</sup>H NMR spectra between chalcone **2a** and compound **3a**, which was isolated as the sole product, clearly indicated the disappearance of characteristic olefinic protons (δ 7.63 and 7.75 ppm) from the prop-2-en-1-one moiety. Furthermore, the <sup>13</sup>C NMR and DEPT, along with the <sup>1</sup>H-<sup>13</sup>C HSQC spectroscopic data of **3a**, revealed the presence of two new quaternary carbons (δ 139.16 and 144.4 ppm) in the absence of two olefinic methine carbons, clearly indicating a successful oxidative cyclization to flavanol. The structure of the pyrano[2,3-*c*]pyrazol-4(2*H*)-one ring system **3a** bearing phenyl substituents at sites N-2 and C-6 was further elucidated via the connectivities based on the through-space correlations from the <sup>1</sup>H-<sup>1</sup>H NOESY spectrum. In this case, distinct NOEs were exhibited between the pyrazole ring proton 3-H (singlet, δ 9.38 ppm) and the neighboring phenyl group 2'(6')-H protons (δ 8.01–8.03 ppm), which confirms their proximity in space. The pyrazole 3-H proton was easily distinguished as it exhibited not only long-range HMBC correlations with neighboring N-2 “pyrrole-like” (δ –167.7 ppm) and N-1 “pyridine-like” (δ –117.0 ppm) nitrogen atoms, but also HMBC correlations with the quaternary carbons C-3a (δ 108.3 ppm) and C-7a (δ 161.2 ppm), respectively. The quaternary carbons C-5 (δ 139.16 ppm) and C-6 (δ 144.4 ppm) were assigned by comparing the long-range correlations obtained from the <sup>1</sup>H-<sup>13</sup>C HMBC and <sup>1</sup>H-<sup>13</sup>C LR-HSQMBC spectra. The most downfield and significantly broadened <sup>1</sup>H signal resonating at δ 9.44 ppm was attributed to the hydroxyl group as it lacked correlations in the HSQC spectra. Finally, by process of elimination, the most downfield <sup>13</sup>C signal resonating at δ 171.8 ppm was confidently assigned to the carbonyl carbon, thus completing our assignment of the pyrano[2,3-*c*]pyrazol-4(2*H*)-one ring system. An in-depth analysis of NMR spectral data showed that the chemical shift values were highly consistent within the flavonol analogues **3a–h**, thus validating the shifts for each position (Table S2).

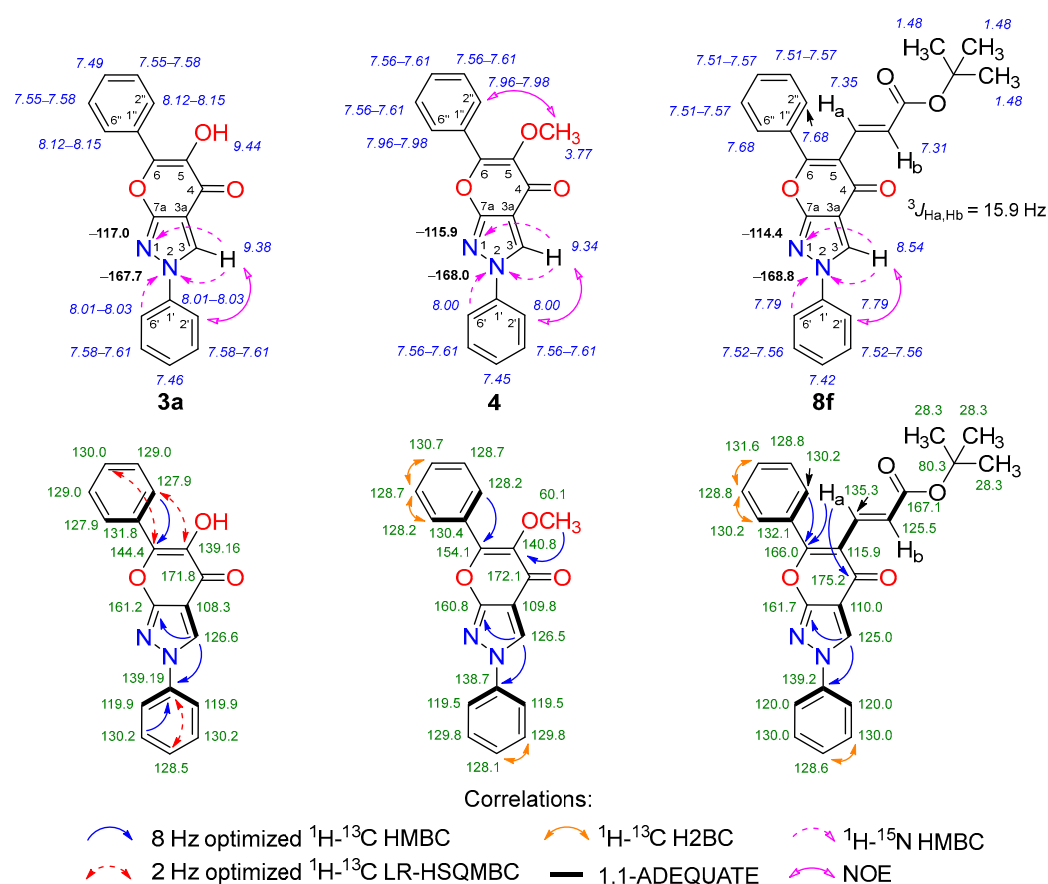


**Figure 3.** Relevant  $^1\text{H}$ - $^{13}\text{C}$  HMBC,  $^1\text{H}$ - $^{13}\text{C}$  LR-HSQMBC,  $^1\text{H}$ - $^{13}\text{C}$  H2BC,  $^1\text{H}$ - $^{15}\text{N}$  HMBC,  $^1\text{H}$ - $^1\text{H}$  NOESY, and 1,1-ADEQUATE correlations, as well as  $^1\text{H}$  NMR (italics),  $^{13}\text{C}$  NMR, and  $^{15}\text{N}$  NMR (bold) chemical shifts of compounds **3a** (DMSO- $d_6$ ), **4** (DMSO- $d_6$ ), and **8f** ( $\text{CDCl}_3$ ).

The presence of a hydroxyl group at site 5 was further confirmed by the conversion of **3a** to *O*-methylated and *O*-triflated derivatives **4** and **7**, respectively. While the structural elucidation of *O*-methylated compound **4** was straightforward and followed the same logical approach as in the case of compounds **3a–h**, additional distinct NOEs were observed between the methoxy group protons ( $\delta$  3.77 ppm) and the neighboring phenyl group 2''(6'')-H protons ( $\delta$  7.96–7.98 ppm). The formation of *O*-triflated derivative **7** was clearly distinguished from the  $^{13}\text{C}$  NMR spectrum, where the  $\text{CF}_3$  group was observed as a quartet at  $\delta$  118.2 ppm ( $q$ ,  $^1J_{\text{CF}} = 320.8$  Hz). Moreover, the  $^{19}\text{F}$  NMR spectrum revealed a chemical shift of the  $\text{CF}_3$  group at  $\delta$  -74.0 ppm, which is in good agreement with the data reported in the literature [54,55]. The triflate intermediate **7** underwent Pd-catalyzed coupling reactions to give derivatives **8a–g**, whose structures were also unambiguously elucidated. For instance, compound **8f** was obtained as an *E*-isomer. The magnitude of the vicinal coupling between the olefinic protons  $\text{H}_a$  ( $\delta$  7.35 ppm) and  $\text{H}_b$  ( $\delta$  7.31 ppm), which exhibited an AB-spin system and appeared as two sets of doublets ( $^3J_{\text{H}_a, \text{H}_b} = 15.9$  Hz), unquestionably confirmed *E*-configuration at the C=C double bond. Lastly, the olefinic protons were easily discriminated as only the proton  $\text{H}_a$  exhibited long-range  $^1\text{H}$ - $^{13}\text{C}$  HMBC correlations with neighboring C-4, C-5, and C-6 quaternary carbons (Figure 3).

The NMR spectral data of compound **3h** with a pyridine moiety at site 6 revealed similar chemical shifts in the pyrano[2,3-*c*]pyrazol-4(2*H*)-one ring system compared with **3a–g**. The  $^1\text{H}$ - $^{15}\text{N}$  HMBC spectrum revealed a new downfield  $^{15}\text{N}$  signal resonating at  $\delta$  -62.2 ppm in addition to N-2 “pyrrole-like” ( $\delta$  -166.9 ppm) and N-1 “pyridine-like” ( $\delta$  -117.1 ppm) nitrogen atoms from the pyrazole moiety. The formation of methylpyridinium iodide **6** via the alkylation of **3h** was unambiguously confirmed from the  $^1\text{H}$ - $^{15}\text{N}$  HMBC and  $^1\text{H}$ - $^1\text{H}$  NOESY spectral data. For instance, distinct NOEs were observed between the

methyl group protons ( $\delta$  4.39 ppm) and the neighboring pyridinium 2''(6'')-H protons ( $\delta$  9.03 ppm). The aforementioned protons revealed strong long-range correlations with the methylpyridinium nitrogen at  $\delta$  -183.3 ppm, which is in good agreement with the data reported in the literature [56].

In the case of compound **5**, which can exist in two resonant forms, the  $^1\text{H}$ - $^{15}\text{N}$  HMBC spectrum revealed a new upfield  $^{15}\text{N}$  signal resonating at  $\delta$  -214.4 ppm. Furthermore, distinct  $^1\text{H}$  and  $^{13}\text{C}$  signals, which appeared to be broadened, were also observed (sites 2'', 3'', 5'', and 6''). Additionally, the key information for the structure elucidation of compounds **3h**, **5**, and **6** was obtained after an in-depth analysis of the long-range correlations in the  $^1\text{H}$ - $^{13}\text{C}$  HMBC,  $^1\text{H}$ - $^{13}\text{C}$  H2BC, and  $^1\text{H}$ - $^{13}\text{C}$  LR-HSQMBC spectra (Figure 4) [57].

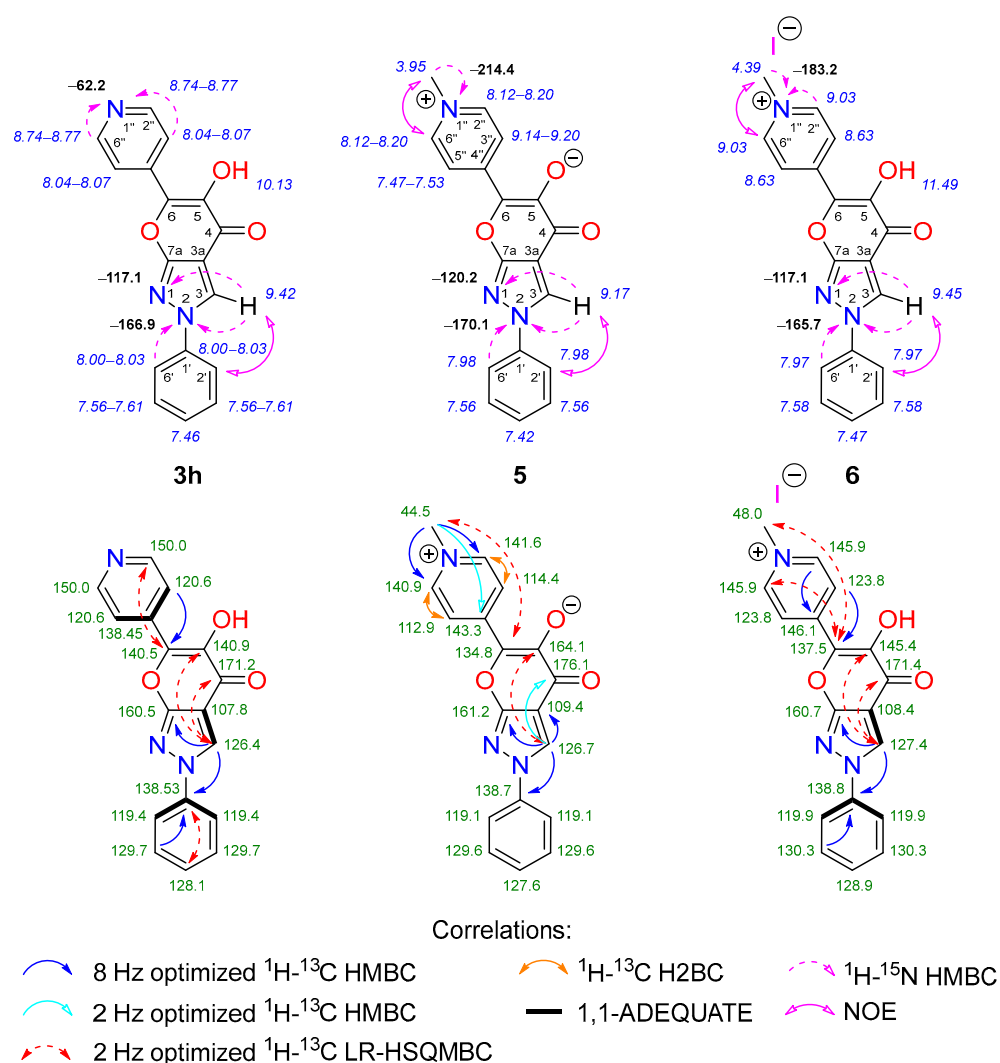
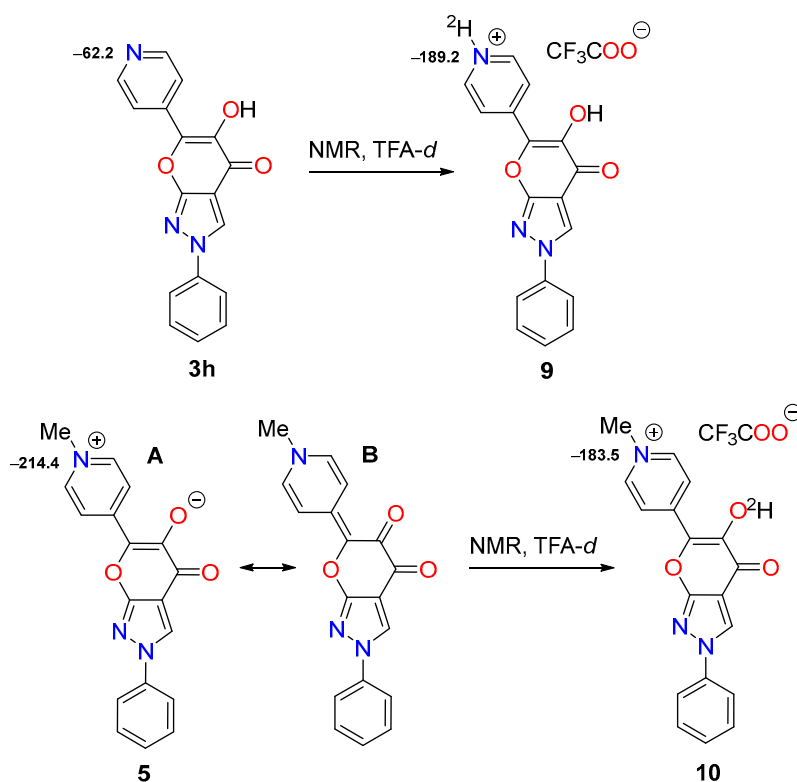


**Figure 4.** Relevant  $^1\text{H}$ - $^{13}\text{C}$  HMBC,  $^1\text{H}$ - $^{13}\text{C}$  LR-HSQMBC,  $^1\text{H}$ - $^{13}\text{C}$  H2BC,  $^1\text{H}$ - $^{15}\text{N}$  HMBC,  $^1\text{H}$ - $^1\text{H}$  NOESY, and 1,1-ADEQUATE correlations, as well as  $^1\text{H}$  NMR (italics),  $^{13}\text{C}$  NMR, and  $^{15}\text{N}$  NMR (bold) chemical shifts of compounds **3h** (DMSO- $d_6$ ), **5** (DMSO- $d_6$ ), and **6** (DMSO- $d_6$ ).

Then, we carried out NMR studies of compounds **3h** and **5** at 25 °C in TFA- $d$  solutions (Scheme 5) to convert them to pyridinium and methylpyridinium trifluoroacetates **9** and **10**, respectively. The  $^{15}\text{N}$  NMR spectral data confirmed that it was easily achieved as “pyridinium-like”  $^{15}\text{N}$  signals comparable to compound **6** resonating at  $\delta$  -189.2 ppm and  $\delta$  -183.2 ppm were observed. Moreover, in the case of compound **10**, which was obtained from compound **5**, the broadening of the  $^1\text{H}$  and  $^{13}\text{C}$  signals was absent.



**Scheme 5.**  $^{15}\text{N}$  NMR (bold) chemical shifts of compounds **3h** ( $\text{DMSO-}d_6$ ), **5** ( $\text{DMSO-}d_6$ ), **9** ( $\text{TFA-}d$ ), and **10** ( $\text{TFA-}d$ ).

### 2.3. Single-Crystal X-ray Diffraction Analysis

The asymmetric molecular structure of compound **5** is shown in Figure 5a. The single crystal is composed of compound **5** solvated with molecules of methanol. The methanol formed hydrogen bonds in the monocystal of **5**, including the hydrogen link to the O(15) (the  $\text{H}\cdots\text{O}$  length is 1.917 Å) (Table S6). The intramolecular hydrogen bond is also observed between the O(15) enolate oxygen and the C(17)–H(17) hydrogen atom (the  $\text{H}\cdots\text{O}$  length is 2.207 Å). The main core of compound **5** consists of the planar pyrano[2,3-*c*]pyrazole ring system, which possesses phenyl and the pyridin-4-yl substituents at N(2) and C(6), respectively. These substituents are slightly distorted from the pyrano[2,3-*c*]pyrazole plane. The phenyl ring is turned approx.  $10^\circ$  and the pyridinyl ring for approx.  $6^\circ$  counterclockwise when looking outward from the core. The N(19)–C(22) bond length of the *N*-methylpyridinium moiety is 1.4737(14) Å (Table S9), and the C(17)–C(18) and C(20)–C(21) bond lengths are 1.3721(15) and 1.3633(16) Å, respectively, and agree with the known bond lengths of the *N*-methylpyridinium salts [58]. All atoms of the pyridine moiety are located in the same plane in agreement with the data reported in the literature [59].

The selected bond lengths and angles of the pyrano[2,3-*c*]pyrazole ring are shown in Tables 1 and 2. The C=O bond length of the pyran-4-one moiety is 1.2265(14) Å which is characteristic of ketone [60]. The C(5)–O(15) bond length [1.2723(13) Å] is shorter than the typical C–O single bond ( $\sim 1.43$  Å) [61], but longer than the typical C=O double bond ( $\sim 1.23$  Å) [62]. It is notable that the C(6)–O(7) bond length [1.4135(12) Å] is longer than that in the O(7)–C(7a) [1.3387(12) Å]. The N(1)–N(2) and N(2)–C(3) bond lengths are 1.3839(12) and 1.3458(14) Å, respectively, and agree with the known bond lengths of pyrazole compounds [63–66]. The sum of the angles between the covalent bonds around the N(2) atom is  $360^\circ$ , which indicates that a *trigonal planar* geometry exists at the  $\text{sp}^2$ -hybridized nitrogen atom. The molecules in the crystal are located in columns made up of asymmetric units held by hydrogen bonds (Figure 5b).

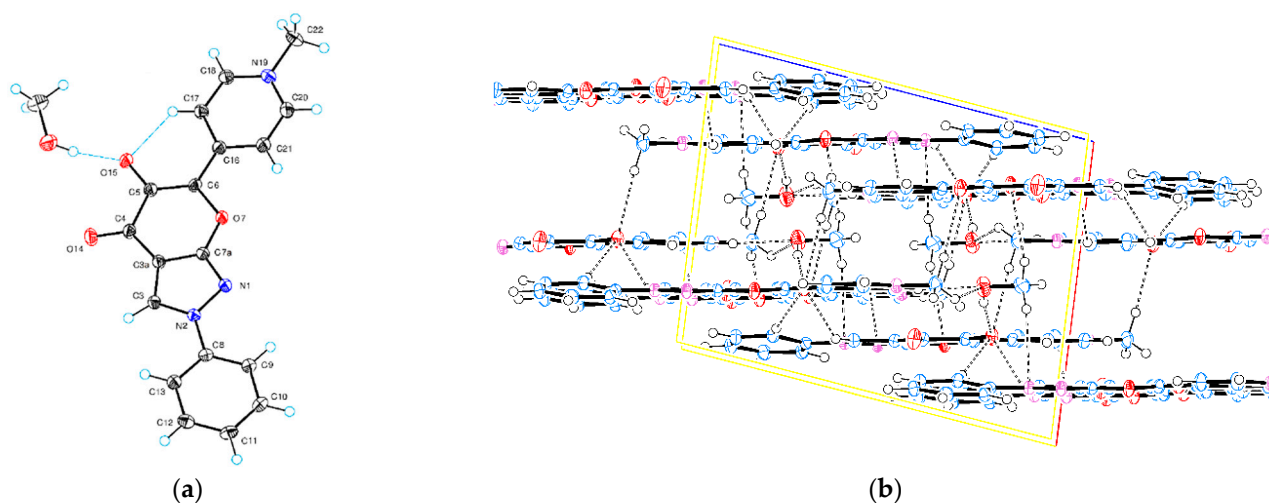


**Figure 5.** ORTEP view of compound 5: (a) asymmetric unit; (b) crystal cell and hydrogen bonds.

**Table 1.** Selected bond lengths [Å] for compound 5.

Atom	Atom	Length/Å	Atom	Atom	Length/Å
N1	N2	1.3839(12)	C4	C5	1.5140(14)
N1	C7A	1.3233(14)	C4	O14	1.2265(14)
N2	C3	1.3458(14)	C5	C6	1.4047(15)
N2	C8	1.4287(13)	C5	O15	1.2723(13)
C3	C3A	1.3842(14)	C6	O7	1.4135(12)
C3A	C4	1.4411(14)	C6	C16	1.4308(14)
C3A	C7A	1.4017(14)	O7	C7A	1.3387(12)

**Table 2.** Selected bond angles [°] for compound 5.

Atom	Atom	Atom	Angle/°	Atom	Atom	Atom	Angle/°
C7A	N1	N2	102.23(8)	O14	C4	C5	120.99(10)
C3	N2	N1	113.26(8)	C6	C5	C4	119.08(9)
C8	N2	N1	119.35(8)	O15	C5	C4	116.91(9)
C8	N2	C3	127.39(9)	O15	C5	C6	124.01(10)
C3A	C3	N2	106.46(9)	O7	C6	C5	123.66(9)
C4	C3A	C3	134.37(10)	C16	C6	C5	125.60(10)
C7A	C3A	C3	104.07(9)	C16	C6	O7	110.74(9)
C7A	C3A	C4	121.56(9)	C7A	O7	C6	116.70(8)
C5	C4	C3A	113.86(9)	C3A	C7A	N1	113.97(9)
O14	C4	C3A	125.15(10)	O7	C7A	N1	120.98(9)

#### 2.4. Optical Investigations

The optical properties of 5-hydroxy-2,6-diphenylpyrano[2,3-*c*]pyrazol-4(2*H*)-ones **3a–h** in various solvents, such as polar protic (MeOH), polar aprotic (THF and DMF), and non-polar (toluene), were investigated by UV–vis spectroscopy; the compounds were also subjected to fluorimetric measurements. The UV–vis electronic absorption spectra of compounds **3a** and **3b** in MeOH showed the absorption maximum in the 337 and 341 nm, respectively (Figure 6a, Table 3, entries 1, 2). The presence of electron-donating substituents

on the phenyl ring of compounds **3c,d** resulted in a bathochromic shift of the longest wavelength absorption transition. The presence of the 4-methoxyphenyl substituent of structure **3c** shifted  $\lambda_{\max}$  upward by 18 nm (Table 3, entry 3), and the presence of the 3,4-dimethoxyphenyl substituent in structure **3d** shifted  $\lambda_{\max}$  upward by 24 nm (Table 3, entry 4) compared to **3a**, respectively. The bathochromic effect of  $\lambda_{\max}$  at 353 nm is also observed in the UV spectra of the naphthalene ring containing compound **3e**, with a significant delocalization of 10- $\pi$  electrons (Table 3, entry 5). Moreover, the replacement of the phenyl ring in the molecular structure of the products by heterocyclic rings, thiophen-2-yl, furan-3-yl, and pyridin-4-yl moieties induced a significant bathochromic shift of the near-ultraviolet band compared to that of compound **3a**. Specifically, the spectra of the compounds **3f**, **3g**, and **3h** contained intense absorption bands with  $\lambda_{\max}$  at 365, 360 and 355 nm, respectively (Table 3, entries 6, 7, 8).

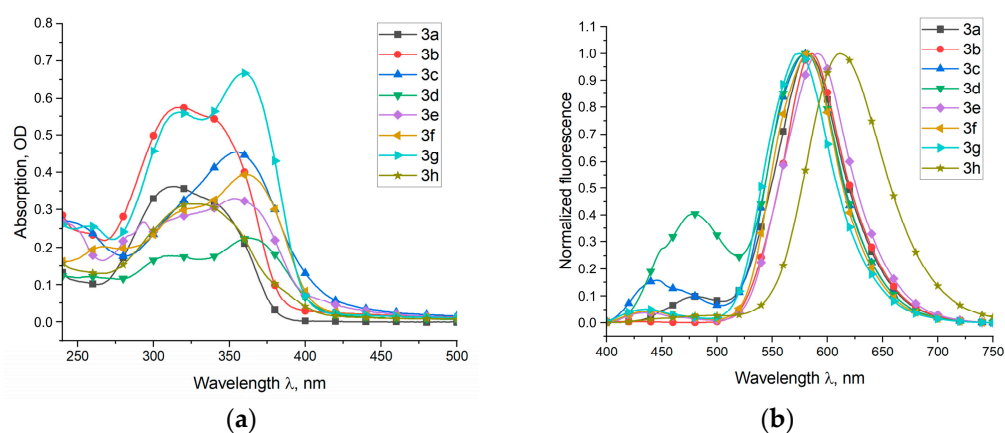


**Figure 6.** (a) UV-vis absorption spectra of compounds **3a–h** in MeOH; (b) fluorescence emission spectra ( $\lambda_{\text{ex}} = 380$  nm) of compounds **3a–h** in MeOH.

The fluorescence spectra of compounds **3a–h** in the MeOH solution contained two well-separated fluorescence bands at around 440 and 590 nm (Figure 6b, Table 3). It is well known that the fluorescence spectra of 3-hydroxyflavone exhibit double emission due to excited-state intramolecular proton transfer (ESIPT) [67–75]. Similarly, in compounds **3a–h**, the proton transfer process (ESIPT) can occur, resulting in the formation of two forms in the excited state: the normal ( $\text{N}^*$ ) and tautomeric (ESIPT product,  $\text{T}^*$ ) forms. For example, the excitation of form  $\text{N-3a}$  leads to the excited state  $\text{N}^*$ , which passes into the product  $\text{T}^*$  by means of proton transfer (Figure 7). The  $\text{T}^*$  form then relaxes to the ground state  $\text{T}$  form and emits fluorescence at a much longer wavelength compared to normal absorption [28,44]. Therefore, the form  $\text{N}^*$  of the normal emission has a Stokes shift of  $8927\text{ cm}^{-1}$ , while the tautomeric product  $\text{T}^*$  has a Stokes shift of  $12491\text{ cm}^{-1}$ .

Measurements of the intensity ratio of the  $\text{N}^*$  and  $\text{T}^*$  bands,  $I_{\text{N}^*}/I_{\text{T}^*}$ , in ESIPT compounds are used for ratiometric detection [70]. A strong effect of group substitution in the compounds **3a–h** was observed on the  $I_{\text{N}^*}/I_{\text{T}^*}$  fluorescence intensity ratio. 4-Chlorophenyl-substituted compound **3b**, compared to the corresponding unsubstituted compound **3a**, showed a dramatically decreased  $I_{\text{N}^*}/I_{\text{T}^*}$  ratio of ~11-fold (Table 3, entry 2). Conversely, the 4-methoxyphenyl-substituted compound **3c** and 3,4-dimethoxyphenyl-substituted compound **3d**, compared to the corresponding compound **3a**, showed increased  $I_{\text{N}^*}/I_{\text{T}^*}$  ratios by ~1.6- and ~4-fold, respectively (Table 3, entries 3,4). In addition, it was found that the corresponding compounds **3e–h**, containing the naphthalen-2-yl, thiophen-2-yl, furan-3-yl, and pyridin-4-yl groups replacing the phenyl group in compound **3a**, caused a decrease in  $I_{\text{N}^*}/I_{\text{T}^*}$  ratios of ~2–3-fold (Table 3, entries 5–8).

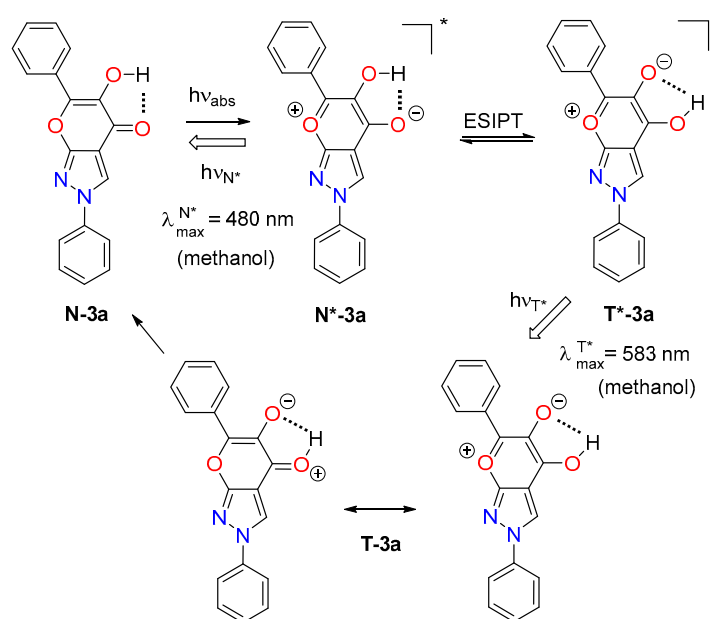


**Figure 7.** Depiction of the ESIPt process in 3a.

**Table 3.** Absorption ( $\lambda_{\text{abs}}$  of the absorption maxima and  $\epsilon$ ), fluorescence emission ( $\lambda_{\text{em}}^{\text{N}^*}$ ,  $\lambda_{\text{em}}^{\text{T}^*}$ , ratio  $I_{\text{N}^*}/I_{\text{T}^*}$  and quantum yield  $\Phi_f$ ) parameters, and Stokes shifts for 3a–h in MeOH ( $^*\lambda_{\text{ex}} = 380 \text{ nm}$ ); sh = shoulder.

Entry	Comp.	$\lambda_{\text{abs}}$ (nm)	$\epsilon \times 10^3$ ( $\text{dm}^3 \text{ mol}^{-1} \text{ cm}^{-1}$ )	$\lambda_{\text{em}}^{\text{N}^*}$ (nm)	$\lambda_{\text{em}}^{\text{T}^*}$ (nm)	$I_{\text{N}^*}/I_{\text{T}^*}$	Stokes Shift ( $\text{cm}^{-1}$ )	$\Phi_f$ (%)	
1	3a	337sh	70.89	482	582	0.102	8927	59.3	
		311	78.45						12491
2	3b	341sh	112.50	428	586	0.009	5961	42.7	
		317	119.51						12261
3	3c	355	93.74	446	582	0.161	5747	13.4	
		320sh	66.27						10987
		240	54.91						
4	3d	361	43.82	479	580	0.406	6824	52.7	
		311	34.60						10459
		261	23.65						
5	3e	353	70.76	435	591	0.043	5340	76.1	
		321sh	60.39						11408
		310sh	57.42						
		293	56.73						
6	3f	245sh	55.59	438	582	0.046	4566	55.8	
		365	80.34						10215
		317sh	59.96						
7	3g	266	41.23	435	575	0.054	4789	42.6	
		360	138.88						10386
		317	116.75						
8	3h	260	53.16	493	611	0.031	7885	13.1	
		355sh	49.99						11802
		329	61.54						

The fluorescence quantum yield ( $\Phi_f$ ) of the solutions was estimated using the integrating sphere method. It appeared that the fluorescence quantum yield was sensitive to

the structure of compounds **3a–h**. For unsubstituted compound **3a**, a high  $\Phi_f$  value was observed at 59.3%. The fluorescence quantum yield of 4-methoxyphenyl-group-containing compound **3c** was low and did not exceed 14%. The highest  $\Phi_f$  value (76.1%) was measured for naphthalen-2-yl-group-containing compound **3e**; the thiophen-2-yl, furan-3-yl, and pyridin-4-yl groups of compounds **3f**, **3g**, and **3h** emitted fluorescence with the observed  $\Phi_f$  values of 55.8%, 42.6%, and 13.1%, respectively. It is notable that 3-hydroxyflavone had low quantum yield values in methanol ( $\Phi_f = 3\%$ ) and DMF ( $\Phi_f = 1.3\%$ ) [70].

Next, the UV–vis electronic absorption spectra of compounds **3a–h** in a polar aprotic solvent, THF, showed the absorption maximum in the 339–362 nm range (Figure 8a, Table 4, entries 1–8). The fluorescence spectra ( $\lambda_{\text{ex}} = 380$  nm) of compounds **3a–h** in the THF solution showed two fluorescence bands at around 441 nm and 591 nm (Figure 8b, Table 4, entries 1–8), which were similar to the bands in MeOH. The inhibition of the ESIPT reaction by protic solvents in 3-hydroxyflavones is associated with the formation of intermolecular H-bonds, which weaken the intramolecular H-bond necessary for the ESIPT reaction [69,74]. Therefore, the relative intensity of the  $N^*$  band was very weak compared to that of the  $T^*$  band for compounds **3a** in THF as an aprotic solvent. Compounds **3c–g**, especially the ones containing methoxyphenyl groups, presented dramatically decreased  $I_{N^*}/I_{T^*}$  ratios in the THF solutions compared to those in MeOH, but the 4-chlorophenyl substituent possessing compound **3b** retained similar  $I_{N^*}/I_{T^*}$  ratios. However, compound **3h** containing the pyridinyl substituent possessed reversed  $I_{N^*}/I_{T^*}$  ratios of 0.221 from 0.031 in MeOH. It is possible that the molecule transferred the corresponding proton to pyridine instead of to the carbonyl group. In this case, the pyridin-4-yl substituent inhibits the proton transfer process (ESIPT).

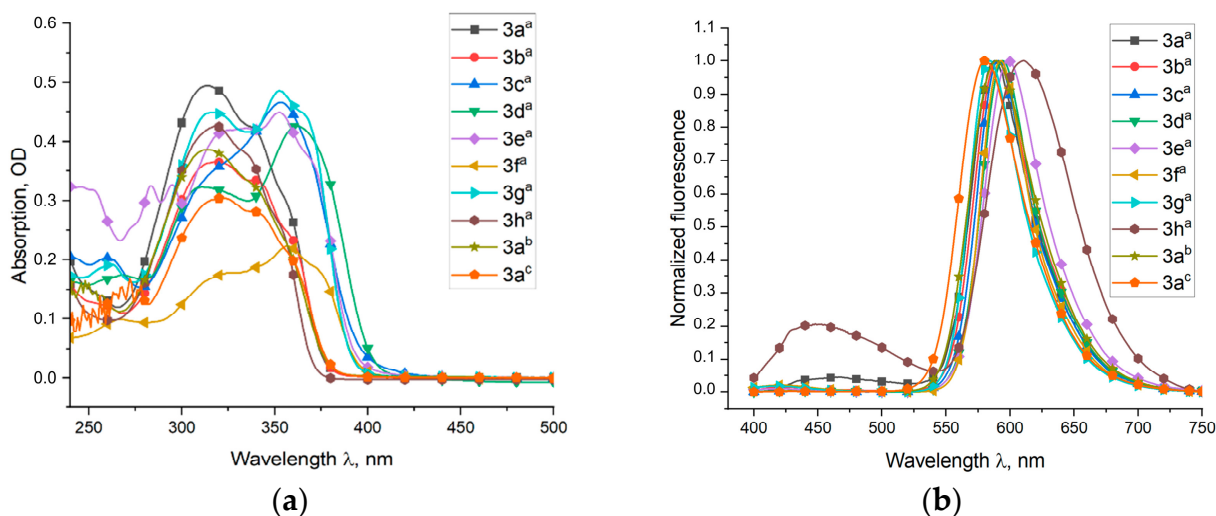


**Figure 8.** (a) UV–vis absorption spectra of compounds **3a–h** in aprotic solvents; (b) fluorescence emission spectra ( $\lambda_{\text{ex}} = 380$  nm) of compounds **3a–h** in aprotic solvents.

The fluorescence spectra of compound **3a** in polar aprotic solvent, DMF, contained two fluorescence bands in the regions of 428 and 589 nm and showed an  $I_{N^*}/I_{T^*}$  ratio of 0.009 (Figure 8b, Table 4, entry 9), while compound **3a** in toluene contained two fluorescence bands in the region of 430 and 589 nm and showed an  $I_{N^*}/I_{T^*}$  ratio of 0.004 (Figure 8b, Table 4, entry 10).

**Table 4.** Absorption ( $\lambda_{\text{abs}}$  absorption maxima and  $\epsilon$ ), fluorescence emission ( $\lambda_{\text{em}}^{\text{N}^*}$ ,  $\lambda_{\text{em}}^{\text{T}^*}$ , ratio  $I_{\text{N}^*}/I_{\text{T}^*}$ , and quantum yield  $\Phi_f$ ) parameters, and Stokes shifts for **3a–h** in aprotic solvents (<sup>a</sup> THF, <sup>b</sup> DMF, and <sup>c</sup> toluene) ( $\lambda_{\text{ex}} = 380$  nm); sh = shoulder.

Entry	Comp.	$\lambda_{\text{abs}}$ (nm)	$\epsilon \times 10^3$ ( $\text{dm}^3 \text{mol}^{-1} \text{cm}^{-1}$ )	$\lambda_{\text{em}}^{\text{N}^*}$ (nm)	$\lambda_{\text{em}}^{\text{T}^*}$ (nm)	$I_{\text{N}^*}/I_{\text{T}^*}$	Stokes Shift ( $\text{cm}^{-1}$ )	$\Phi_f$ (%)																																																																																																																																	
1	3a <sup>a</sup>	339sh	58.67	466	588	0.014	8039	59.2																																																																																																																																	
		315	69.15						12492	2	3b <sup>a</sup>	339	49.24	428	590	0.019	6134	75.5	317	53.74	6134	240	22.77		3	3c <sup>a</sup>	353	69.71	428	591	0.005	4964	19.2	318sh	52.84	11408	260	30.30		4	3d <sup>a</sup>	362	58.61	429	594	0.006	4314	39.6	311	44.19	10789	268	23.99		5	3e <sup>a</sup>	352	63.18	416	598	0.012	4371	50.6	334sh	59.61	11687	295	46.02		283	45.73		6	3f <sup>a</sup>	357	35.90	423	593	0.023	43,701	41.2	327sh	28.75	11148	266	15.87		7	3g <sup>a</sup>	352	82.58	421	584	0.020	4656	55.0	317	75.99	11286	262	32.57		8	3h <sup>a</sup>	351sh	40.75	442	610	0.221	5866	30.1	335sh	57.39	12097	319	64.62		9	3a <sup>b</sup>	338sh	64.22	428	589	0.009	6221	45.5	315	75.82	12608	10	3a <sup>c</sup>	357sh	43.31	430	581	0.004	4755
2	3b <sup>a</sup>	339	49.24	428	590	0.019	6134	75.5																																																																																																																																	
		317	53.74						6134																																																																																																																																
		240	22.77																																																																																																																																						
3	3c <sup>a</sup>	353	69.71	428	591	0.005	4964	19.2																																																																																																																																	
		318sh	52.84						11408																																																																																																																																
		260	30.30																																																																																																																																						
4	3d <sup>a</sup>	362	58.61	429	594	0.006	4314	39.6																																																																																																																																	
		311	44.19						10789																																																																																																																																
		268	23.99																																																																																																																																						
5	3e <sup>a</sup>	352	63.18	416	598	0.012	4371	50.6																																																																																																																																	
		334sh	59.61						11687																																																																																																																																
		295	46.02																																																																																																																																						
		283	45.73																																																																																																																																						
6	3f <sup>a</sup>	357	35.90	423	593	0.023	43,701	41.2																																																																																																																																	
		327sh	28.75						11148																																																																																																																																
		266	15.87																																																																																																																																						
7	3g <sup>a</sup>	352	82.58	421	584	0.020	4656	55.0																																																																																																																																	
		317	75.99						11286																																																																																																																																
		262	32.57																																																																																																																																						
8	3h <sup>a</sup>	351sh	40.75	442	610	0.221	5866	30.1																																																																																																																																	
		335sh	57.39						12097																																																																																																																																
		319	64.62																																																																																																																																						
9	3a <sup>b</sup>	338sh	64.22	428	589	0.009	6221	45.5																																																																																																																																	
		315	75.82						12608																																																																																																																																
10	3a <sup>c</sup>	357sh	43.31	430	581	0.004	4755	67.7																																																																																																																																	
		338	57.48						10800																																																																																																																																
		322	62.27																																																																																																																																						

Derivative **4** with the 5-MeO substituent had an electron spectrum very close to its analog **3a** (absorption maximum 306 nm and 302 nm, respectively) (Figure S1a). In the fluorescence spectrum of compound **4** in THF solution, two bands were observed at 475 and 582 nm with insignificant fluorescence ( $\Phi_f < 0.1\%$ ) (Figure S1b, Table S12, entry 1). Ormson et al. reported that the fluorescence quantum yield for 3-hydroxyflavone is much greater than for the corresponding methoxy compounds and their fluorescence lifetimes are longer [76].

The UV–vis absorption and fluorescence emission spectra of 5-substituted 2,6-diphenyl pyrano[2,3-*c*]pyrazol-4(2*H*)-ones **8a,f,g** in THF were also investigated (Figure S1a, Table S12). The absorption maximum of compounds **8a,f,g** was in the range from 297 to 302 nm (near-ultraviolet region). None of the investigated compounds **8a,f,g** exhibited an absorption in the visible portion of the electronic spectrum. Upon excitation at 340 nm in THF solution, compounds **8a,f,g** showed fluorescence emission maxima ( $\lambda_{\text{em}}$ ) at around 593–603 nm, although fluorescence was weak (Figure S1b, Table S12). Compound **8a** derived from 2,6-diphenylpyrano[2,3-*c*]pyrazol-4(2*H*)-one containing 5-phenyl substituent produced a low quantum yield ( $\Phi_f = 1\%$ ) (Table S12, entry 2); for compounds **8f** and **8g**, the

observed  $\Phi_f$  had a negligible value of only <0.1% (Table S12, entries 3, 4). All compounds **8a,f,g** possessed very high values of Stokes shift of  $\sim\Delta\nu = 16000$  nm.

Finally, we investigated the UV–vis spectra of compounds **5** and **6**. In a polar aprotic solvent, THF, both compounds showed the same absorption maximum in the 528 nm (Figure 9, Table 5). The versatility of derivatives of zwitterionic chromophore, including pyran compounds, in synthetic and material applications, has been well documented [77–79].

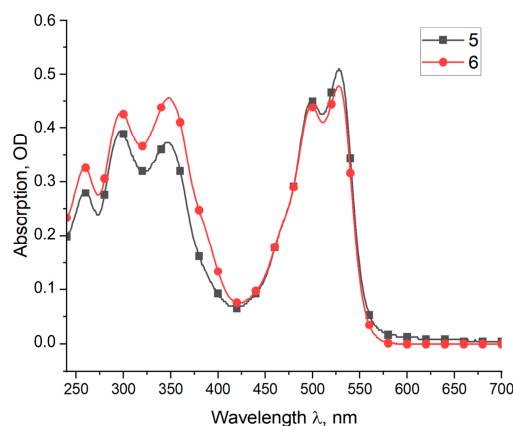


**Figure 9.** UV–vis electronic absorption spectra of compounds **5** and **6** in THF.

**Table 5.** Absorption ( $\lambda_{\text{abs}}$  absorption maxima and  $\epsilon$ ) of compounds **5** and **6** in THF.

Entry	Comp.	$\lambda_{\text{abs}}$ (nm)	$\epsilon \times 10^3$ (dm <sup>3</sup> mol <sup>-1</sup> cm <sup>-1</sup> )
1	5	528	0.55
		499	0.48
		346	0.39
		299	0.42
		261	0.30
2	6	528	0.54
		499	0.49
		348	0.52
		297	0.49
		261	0.37

### 3. Materials and Methods

#### 3.1. General

All the chemicals and solvents were purchased from common commercial suppliers. Diffraction data were collected on a Rigaku, XtaLAB Synergy, Dualflex, HyPix diffractometer (Rigaku Corporation, Tokyo, Japan). The crystals were kept at 150.0(1) K while collecting the data. Using Olex2, the structure was solved with the ShelXT structure solution program using intrinsic phasing and refined with the olex2.refine refinement package using Gauss–Newton minimization. The <sup>1</sup>H, <sup>13</sup>C, and <sup>15</sup>N NMR spectra were recorded in CDCl<sub>3</sub> or DMSO-*d*<sub>6</sub> at 25 °C on a Bruker Avance III 700 (700 MHz for <sup>1</sup>H, 176 MHz for <sup>13</sup>C, and 71 MHz for <sup>15</sup>N) spectrometer (Bruker BioSpin GmbH, Rheinstetten, Germany) equipped with a 5 mm TCI <sup>1</sup>H-<sup>13</sup>C/<sup>15</sup>N/D z-gradient cryoprobe. The chemical shifts were referenced to tetramethylsilane (TMS) and expressed in ppm. The <sup>15</sup>N NMR spectra were referenced against neat, external nitromethane (coaxial capillary). <sup>19</sup>F NMR spectrum (376 MHz) was obtained on a Bruker Avance III 400 instrument (Bruker BioSpin AG, Faellanden, Switzerland) with absolute referencing via  $\delta$  ratio. The FT-IR spectra were recorded by ATR method on either a Bruker Vertex 70v spectrometer (Bruker Optik GmbH, Ettlingen, Germany) with an integrated Platinum ATR accessory or on a Bruker Tensor 27 spectrometer (Bruker Optik GmbH, Ettlingen, Germany) using KBr pellets. The melting points of the crystalline compounds were measured in open capillary tubes with a Buchi

M 565 apparatus and are uncorrected. Mass spectra were obtained using a Shimadzu LCMS-2020 (ESI<sup>+</sup>) spectrometer (Shimadzu Corporation, Kyoto, Japan). High-resolution mass spectra (HRMS) were measured using a Bruker MicrOTOF-Q III (ESI<sup>+</sup>) apparatus (Bruker Daltonik GmbH, Bremen, Germany). All the reactions were performed in oven-dried glassware with magnetic stirring. The reaction progress was monitored by TLC analysis on Macherey-Nagel<sup>TM</sup> ALUGRAM<sup>®</sup> Xtra SIL G/UV254 plates (Macherey-Nagel GmbH & Co. KG, Düren, Germany) which were visualized by UV light (254 and 365 nm wavelengths). The compounds were purified by flash chromatography in glass columns (stationary phase of silica gel, high-purity grade of 9385, pore size of 60 Å, and particle size of 230–400 mesh, supplied by Sigma-Aldrich; Merck KGaA, Darmstadt, Germany). The UV-vis spectra were recorded on a Shimadzu 2600 UV/vis spectrometer (Shimadzu Corporation, Japan). The fluorescence spectra were recorded on an FL920 fluorescence spectrometer from Edinburgh Instruments (Edinburgh Analytical Instruments Limited, Edinburgh, UK). The PL quantum yields were determined from dilute solutions by an absolute method using the Edinburgh Instruments integrating sphere excited with a Xe lamp. The optical densities of the sample solutions were ensured to be below 0.1 to avoid reabsorption effects. All the optical measurements were performed at room temperature under ambient conditions. The following abbreviations are used in reporting the NMR data: Ph, phenyl; Pyr, pyridine; Pz, pyrazole; Naph, naphthalene; and Th, thiophene. The <sup>1</sup>H, <sup>13</sup>C, and <sup>1</sup>H-<sup>15</sup>N HMBC NMR spectra, as well as the HRMS data of the new compounds, are provided in Figures S2–S81 of the Supplementary Material. Crystallographic data have been deposited at the Cambridge Crystallographic Data Centre with CCDC reference number 2287991 for 6-(1-methylpyridin-1-ium-4-yl)-4-oxo-2-phenyl-2,4-dihydropyrano[2,3-*c*]pyrazol-5-olate (**5**); formula C<sub>19</sub>H<sub>17</sub>N<sub>3</sub>O<sub>4</sub>; unit cell parameters: a 10.39395(17) b 12.15508(19) c 13.08074(18), space group P21/*c*.

### 3.2. Synthetic Procedures

Compounds **2a–c** and **2e–h** were synthesized in accordance with the procedure described in ref. [44].

#### 3.2.1. (2*E*)-3-(3,4-Dimethoxyphenyl)-1-(3-hydroxy-1-phenyl-1*H*-pyrazol-4-yl)prop-2-en-1-one (**2d**)

The compound was synthesized in accordance with the procedure described in ref. [44] using 3,4-dimethoxybenzaldehyde. Orange solid. Yield 67% (2349 mg); m.p. 225–226 °C. <sup>1</sup>H NMR (700 MHz, DMSO-*d*<sub>6</sub>): δ<sub>H</sub> ppm 3.82 (s, 3H, 4-OCH<sub>3</sub>), 3.84 (s, 3H, 3-OCH<sub>3</sub>), 7.05 (d, *J* = 8.1 Hz, 1H, CPh 5-H), 7.33 (t, *J* = 7.4 Hz, 1H, NPh 4-H), 7.34–7.37 (m, 2H, CPh 2,6-H), 7.52 (t, *J* = 7.9 Hz, 2H, NPh 3,5-H), 7.57 (d, *J* = 15.6 Hz, 1H, C(O)CHCH), 7.66 (d, *J* = 15.6 Hz, 1H, C(O)CHCH), 7.84 (d, *J* = 7.8 Hz, 2H, NPh 2,6-H), 9.12 (s, 1H, Pz 5-H), 11.07 (s, 1H, OH). <sup>13</sup>C NMR (176 MHz, DMSO-*d*<sub>6</sub>): δ<sub>C</sub> ppm 55.6 (4-OCH<sub>3</sub>), 55.7 (3-OCH<sub>3</sub>), 111.0 (Pz C-4), 111.3 (CPh C-2), 111.8 (CPh C-5), 118.1 (NPh C-2,6), 121.8 (C(O)CHCH), 122.7 (CPh C-6), 126.6 (NPh C-4), 127.5 (CPh C-1), 129.6 (NPh C-3,5), 131.5 (Pz C-5), 138.9 (NPh C-1), 142.0 (C(O)CHCH), 149.0 (CPh C-3), 151.1 (CPh C-4), 162.0 (Pz C-3), 182.9 (C=O). <sup>15</sup>N NMR (71 MHz, DMSO-*d*<sub>6</sub>): δ<sub>N</sub> ppm –182.3 (Pz N-1), –118.3 (Pz N-2). IR (ν<sub>max</sub>, cm<sup>–1</sup>): 3118, 2932, 1652 (C=O), 1586, 1510, 1451, 1218, 1026, 977, 742, 679. HRMS (ESI<sup>+</sup>) for C<sub>20</sub>H<sub>18</sub>N<sub>2</sub>NaO<sub>4</sub> ([M + Na]<sup>+</sup>) calcd 373.1159, found 373.1162.

#### 3.2.2. General Procedure for the Synthesis of **3a–h**

To a solution of **2a–h** (1 mmol) in EtOH (5 mL) at –10 °C, aq. NaOH (20%, 1 mL, 5 mmol) was added; the reaction mixture was cooled down to –25 °C and H<sub>2</sub>O<sub>2</sub> 30% (0.51 mL, 5 mmol) was added dropwise. The reaction mixture was stirred for 2 h and at room temperature for another 16 h. The solids were filtered off, washed with warm water, cold MeOH, and ether, and dried. The product was recrystallized from ACN.

5-Hydroxy-2,6-diphenylpyrano[2,3-*c*]pyrazol-4(2*H*)-one (**3a**). Off white solid; yield 58% (177 mg); m.p. 183–184 °C. <sup>1</sup>H NMR (700 MHz, DMSO-*d*<sub>6</sub>): δ<sub>H</sub> ppm 7.46 (t, *J* = 7.4 Hz, 1H, NPh 4-H),

7.49 (t,  $J = 7.4$  Hz, 1H, 6-CPh 4-H), 7.55–7.58 (m, 2H, 6-CPh 3,5-H), 7.58–7.61 (m, 2H, NPh 3,5-H), 8.01–8.03 (m, 2H, NPh 2,6-H), 8.13–8.14 (m, 2H, 6-CPh 2,6-H), 9.38 (s, 1H, 3-H), 9.44 (s, 1H, OH).  $^{13}\text{C}$  NMR (176 MHz, DMSO- $d_6$ ):  $\delta_{\text{C}}$  ppm 108.3 (C-3a), 119.9 (NPh C-2,6), 126.6 (C-3), 127.9 (6-CPh C-2,6), 128.5 (NPh C-4), 129.0 (6-CPh C-3,5), 130.0 (6-CPh C-4), 130.2 (NPh C-3,5), 131.8 (6-CPh C-1), 139.16 (C-5), 139.19 (NPh C-1), 144.4 (C-6), 161.2 (C-7a), 171.8 (C-4).  $^{15}\text{N}$  NMR (71 MHz, DMSO- $d_6$ ):  $\delta_{\text{N}}$  ppm  $-167.7$  (N-2),  $-117.0$  (N-1). IR ( $\nu_{\text{max}}$ ,  $\text{cm}^{-1}$ ): 3110, 3062, 2920, 2850, 1679 (C=O), 1568, 1489, 1199, 1110, 913, 832, 761, 696. HRMS (ESI $^{+}$ ) for  $\text{C}_{18}\text{H}_{12}\text{N}_2\text{NaO}_3$  ([M + Na] $^{+}$ ) calcd 327.0740, found 327.0740.

**6-(4-Chlorophenyl)-5-hydroxy-2-phenylpyrano[2,3-*c*]pyrazol-4(2H)-one (3b).** Light yellow solid; yield 63% (213 mg); m.p. 262–263 °C.  $^1\text{H}$  NMR (700 MHz, DMSO- $d_6$ ):  $\delta_{\text{H}}$  ppm 7.45 (t,  $J = 7.3$  Hz, 1H, NPh 4-H), 7.58 (t,  $J = 7.8$  Hz, 2H, NPh 3,5-H), 7.62 (d,  $J = 8.6$  Hz, 2H, 6-CPh 3,5-H), 8.01 (d,  $J = 7.9$  Hz, 2H, NPh 2,6-H), 8.15 (d,  $J = 8.6$  Hz, 2H, 6-CPh 2,6-H), 9.38 (s, 1H, 3-H), 9.70 (s, 1H, OH).  $^{13}\text{C}$  NMR (176 MHz, DMSO- $d_6$ ):  $\delta_{\text{C}}$  ppm 107.9 (C-3a), 119.5 (NPh C-2,6), 126.3 (C-3), 128.1 (NPh C-4), 128.6 (6-CPh C-3,5), 129.1 (6-CPh C-2,6), 129.8 (NPh C-3,5), 130.2 (6-CPh C-1), 134.1 (6-CPh C-4), 138.7 (NPh C-1), 139.1 (C-5), 142.7 (C-6), 160.6 (C-7a), 171.3 (C-4).  $^{15}\text{N}$  NMR (71 MHz, DMSO- $d_6$ ):  $\delta_{\text{N}}$  ppm  $-167.5$  (N-2),  $-117.2$  (N-1). IR ( $\nu_{\text{max}}$ ,  $\text{cm}^{-1}$ ): 3348, 3289, 3100, 1645 (C=O), 1576, 1495, 1442, 1098, 825, 752, 679. HRMS (ESI $^{+}$ ) for  $\text{C}_{18}\text{H}_{11}\text{ClN}_2\text{NaO}_3$  ([M + Na] $^{+}$ ) calcd 361.0350, found 361.0350.

**5-Hydroxy-6-(4-methoxyphenyl)-2-phenylpyrano[2,3-*c*]pyrazol-4(2H)-one (3c).** Yellow solid; yield 51% (171 mg); m.p. 263–264 °C.  $^1\text{H}$  NMR (700 MHz, DMSO- $d_6$ ):  $\delta_{\text{H}}$  ppm 3.85 (s, 3H, CH $_3$ ), 7.12–7.13 (m, 2H, 6-CPh 3,5-H), 7.45 (t,  $J = 7.4$  Hz, 1H, NPh 4-H), 7.57–7.60 (m, 2H, NPh 3,5-H), 8.00–8.02 (m, 2H, NPh 2,6-H), 8.09–8.12 (m, 2H, 6-CPh 2,6-H), 9.27 (s, 1H, 3-H), 9.36 (s, 1H, OH).  $^{13}\text{C}$  NMR (176 MHz, DMSO- $d_6$ ):  $\delta_{\text{C}}$  ppm 55.3 (CH $_3$ ), 107.9 (C-3a), 114.2 (6-CPh C-3,5), 119.4 (NPh C-2,6), 123.6 (6-CPh C-1), 126.0 (C-3), 128.0 (NPh C-4), 129.2 (6-CPh C-2,6), 129.8 (NPh C-3,5), 137.8 (C-5), 138.8 (NPh C-1), 144.4 (C-6), 160.2 (6-CPh C-4), 160.7 (C-7a), 171.2 (C-4).  $^{15}\text{N}$  NMR (71 MHz, DMSO- $d_6$ ):  $\delta_{\text{N}}$  ppm  $-168.3$  (N-2). IR ( $\nu_{\text{max}}$ ,  $\text{cm}^{-1}$ ): 3286, 3134, 1642 (C=O), 1580, 1509, 1441, 1256, 1108, 821, 748, 680. HRMS (ESI $^{+}$ ) for  $\text{C}_{19}\text{H}_{14}\text{N}_2\text{NaO}_4$  ([M + Na] $^{+}$ ) calcd 357.0846, found 357.0841.

**6-(3,4-Dimethoxyphenyl)-5-hydroxy-2-phenylpyrano[2,3-*c*]pyrazol-4(2H)-one (3d).** Orange solid; yield 67% (245 mg); m.p. 252–253 °C.  $^1\text{H}$  NMR (700 MHz, DMSO- $d_6$ ):  $\delta_{\text{H}}$  ppm 3.84 (s, 3H, 6-CPh 3-OCH $_3$ ), 3.85 (s, 3H, 6-CPh 4-OCH $_3$ ), 7.15 (d,  $J = 8.7$  Hz, 1H, 6-CPh 5-H), 7.45 (t,  $J = 7.4$  Hz, 1H, NPh 4-H), 7.58 (t,  $J = 8.0$  Hz, 2H, NPh 3,5-H), 7.71 (d,  $J = 2.1$  Hz, 1H, 6-CPh 2-H), 7.78 (dd,  $J = 8.6, 2.1$  Hz, 1H, 6-CPh 6-H), 8.02 (d,  $J = 7.7$  Hz, 2H, NPh 2,6-H), 9.28 (s, 1H, OH), 9.35 (s, 1H, 3-H).  $^{13}\text{C}$  NMR (176 MHz, DMSO- $d_6$ ):  $\delta_{\text{C}}$  ppm 55.6 (6-CPh 3,4-OCH $_3$ ), 107.8 (C-3a), 110.7 (6-CPh C-2), 111.5 (6-CPh C-5), 119.4 (NPh C-2,6), 121.3 (6-CPh C-6), 123.7 (6-CPh C-1), 126.0 (C-3), 128.0 (NPh C-4), 129.8 (NPh C-3,5), 137.9 (C-5), 138.8 (NPh C-1), 144.3 (C-6), 148.3 (6-CPh C-3), 150.0 (6-CPh C-4), 160.6 (C-7a), 171.1 (C-4).  $^{15}\text{N}$  NMR (71 MHz, DMSO- $d_6$ ):  $\delta_{\text{N}}$  ppm  $-168.2$  (N-2),  $-117.3$  (N-1). IR ( $\nu_{\text{max}}$ ,  $\text{cm}^{-1}$ ): 3281, 2963, 1632 (C=O), 1583, 1515, 1439, 1106, 754, 657. HRMS (ESI $^{+}$ ) for  $\text{C}_{20}\text{H}_{16}\text{N}_2\text{NaO}_5$  ([M + Na] $^{+}$ ) calcd 387.0951, found 387.0953.

**5-Hydroxy-6-(naphthalen-2-yl)-2-phenylpyrano[2,3-*c*]pyrazol-4(2H)-one (3e).** Yellow solid; yield 32% (113 mg); m.p. 256–257 °C.  $^1\text{H}$  NMR (700 MHz, DMSO- $d_6$ ):  $\delta_{\text{H}}$  ppm 7.46 (t,  $J = 7.4$  Hz, 1H, NPh 4-H), 7.59–7.63 (m, 4H, NPh 3,5-H and Naph 6,7-H), 7.99 (d,  $J = 7.8$  Hz, 1H, Naph 5-H), 8.04 (d,  $J = 7.9$  Hz, 2H, NPh 2,6-H), 8.06–8.09 (m, 1H, Naph 4-H), 8.09–8.10 (m, 1H, Naph 8-H), 8.27 (dd,  $J = 8.7, 1.8$  Hz, 1H, Naph 3-H), 8.71 (s, 1H, Naph 1-H), 9.41 (s, 1H, 3-H), 9.59 (s, 1H, OH).  $^{13}\text{C}$  NMR (176 MHz, DMSO- $d_6$ ):  $\delta_{\text{C}}$  ppm 107.8 (C-3a), 119.3 (NPh C-2,6), 124.3 (Naph C-3), 126.1 (C-3), 126.7 (Naph C-7), 127.38 (Naph C-1 and Naph C-6), 127.44 (Naph C-5), 127.82 (Naph C-4), 128.01 (NPh C-4), 128.76 (Naph C-8), 128.79 (Naph C-2), 129.7 (NPh C-3,5), 132.4 (Naph C-8a), 132.9 (Naph C-4a), 138.7 (NPh C-1), 139.0 (C-5), 143.8 (C-6), 160.7 (C-7a), 171.2 (C-4).  $^{15}\text{N}$  NMR (71 MHz, DMSO- $d_6$ ):  $\delta_{\text{N}}$  ppm  $-167.7$  (N-2),  $-117.4$  (N-1). IR ( $\nu_{\text{max}}$ ,  $\text{cm}^{-1}$ ): 3240, 1629 (C=O), 1576, 1564, 1441, 1386, 1216, 1096, 753, 685. HRMS (ESI $^{+}$ ) for  $\text{C}_{22}\text{H}_{14}\text{N}_2\text{NaO}_3$  ([M + Na] $^{+}$ ) calcd 377.0897, found 377.0908.

**5-Hydroxy-2-phenyl-6-(thiophen-2-yl)pyrano[2,3-c]pyrazol-4(2H)-one (3f).** Yellow solid; yield 62% (193 mg); m.p. 187–188 °C.  $^1\text{H}$  NMR (700 MHz, DMSO- $d_6$ ):  $\delta_{\text{H}}$  ppm 7.29 (dd,  $J = 5.0, 3.8$  Hz, 1H, Th 5-H), 7.44–7.46 (m, 1H, NPh 4-H), 7.57–7.60 (m, 2H, NPh 3,5-H), 7.87 (dd,  $J = 3.8, 1.2$  Hz, 1H, Th 3-H), 7.88 (dd,  $J = 5.0, 1.2$  Hz, 1H, Th 4-H), 8.00–8.02 (m, 2H, NPh 2,6-H), 9.35 (s, 1H, 3-H), 10.12 (s, 1H, OH).  $^{13}\text{C}$  NMR (176 MHz, DMSO- $d_6$ ):  $\delta_{\text{C}}$  ppm 108.1 (C-3a), 119.3 (NPh C-2,6), 126.1 (C-3), 127.66 (Th C-3), 127.70 (Th C-5), 127.9 (NPh C-4), 129.6 (NPh C-3,5), 130.4 (Th C-4), 132.3 (Th C-2), 136.5 (C-5), 138.6 (NPh C-1), 141.9 (C-6), 160.2 (C-7a), 170.4 (C-4).  $^{15}\text{N}$  NMR (71 MHz, DMSO- $d_6$ ):  $\delta_{\text{N}}$  ppm –168.6 (N-2), –117.2 (N-1). IR ( $\nu_{\text{max}}$ ,  $\text{cm}^{-1}$ ): 3259, 3113, 1629 (C=O), 1575, 1503, 1217, 1103, 826, 753, 685. HRMS (ESI $^+$ ) for  $\text{C}_{16}\text{H}_{10}\text{N}_2\text{NaO}_3\text{S}$  ( $[\text{M} + \text{Na}]^+$ ) calcd 333.0304, found 333.0309.

**6-(Furan-3-yl)-5-hydroxy-2-phenylpyrano[2,3-c]pyrazol-4(2H)-one (3g).** Beige solid; yield 30% (89 mg); m.p. 228–229 °C.  $^1\text{H}$  NMR (700 MHz, DMSO- $d_6$ ):  $\delta_{\text{H}}$  ppm 6.78 (dd,  $J = 3.4, 1.7$  Hz, 1H, Furanyl 5-H), 7.23 (d,  $J = 3.4$  Hz, 1H, Furanyl 4-H), 7.45 (t,  $J = 7.4$  Hz, 1H, NPh 4-H), 7.59 (t,  $J = 7.9$  Hz, 2H, NPh 3,5-H), 8.00 (d,  $J = 7.8$  Hz, 2H, NPh 2,6-H), 8.02 (d,  $J = 1.0$  Hz, 1H, Furanyl 2-H), 9.36 (s, 1H, 3-H), 9.86 (s, 1H, OH).  $^{13}\text{C}$  NMR (176 MHz, DMSO- $d_6$ ):  $\delta_{\text{C}}$  ppm 108.2 (C-3a), 112.7 (Furanyl C-5), 114.5 (Furanyl C-4), 119.3 (NPh C-2,6), 126.1 (C-3), 127.9 (NPh C-4), 129.7 (NPh C-3,5), 136.9 (C-5), 138.0 (Furanyl C-3), 138.6 (NPh C-1), 144.0 (C-6), 144.9 (Furanyl C-2), 160.2 (C-7a), 170.3 (C-4).  $^{15}\text{N}$  NMR (71 MHz, DMSO- $d_6$ ):  $\delta_{\text{N}}$  ppm –168.4 (N-2), –117.1 (N-1). IR ( $\nu_{\text{max}}$ ,  $\text{cm}^{-1}$ ): 3246, 3138, 2957, 2856, 1633 (C=O), 1576, 1483, 1221, 1124, 934, 845, 755, 681. HRMS (ESI $^+$ ) for  $\text{C}_{16}\text{H}_{10}\text{N}_2\text{NaO}_4$  ( $[\text{M} + \text{Na}]^+$ ) calcd 317.0533, found 317.0534.

**5-Hydroxy-2-phenyl-6-(pyridin-4-yl)pyrano[2,3-c]pyrazol-4(2H)-one (3h).** Yellow solid; yield 53% (163 mg); m.p. 298–299 °C.  $^1\text{H}$  NMR (700 MHz, DMSO- $d_6$ )  $\delta$  7.45–7.48 (m, 1H, Ph 4-H), 7.56–7.61 (m, 2H, Ph 3,5-H), 8.00–8.03 (m, 2H, Ph 2,6-H), 8.04–8.07 (m, 2H, Pyr 3,5-H), 8.74–8.77 (m, 2H, Pyr 2,4-H), 9.41 (s, 1H, 3-H), 10.13 (s, 1H, OH).  $^{13}\text{C}$  NMR (176 MHz, DMSO- $d_6$ )  $\delta$  107.8 (C-3a), 119.4 (Ph C-2,6), 120.6 (Pyr C-3,5), 126.4 (C-3), 128.1 (Ph C-4), 129.7 (Ph C-3,5), 138.45 (Pyr C-4), 138.53 (Ph C-1), 140.5 (C-6), 140.9 (C-5), 150.0 (Pyr C-2,6), 160.5 (C-7a), 171.2 (C-4).  $^{15}\text{N}$  NMR (71 MHz, DMSO- $d_6$ ):  $\delta_{\text{N}}$  ppm –166.9 (N-2), –117.1 (N-1), –62.2 (Pyr N). IR ( $\nu_{\text{max}}$ ,  $\text{cm}^{-1}$ ): 3112, 3087, 1648 (C=O), 1571, 1500, 1442, 1228, 1026, 834, 754, 629. HRMS (ESI $^+$ ) for  $\text{C}_{17}\text{H}_{11}\text{N}_3\text{O}_3$  ( $[\text{M} + \text{H}]^+$ ) calcd 306.0873, found 306.0871.

### 3.2.3. Procedure for the Synthesis of 5-Methoxy-2,6-diphenylpyrano[2,3-c]pyrazol-4(2H)-one (4)

To a solution of **3a** (304 mg, 1 mmol) in dioxane (30 mL)  $\text{Cs}_2\text{CO}_3$  (0.65 g, 2 mmol) and MeI (0.07 mL, 1.1 mmol) were added. The reaction mixture was stirred at 40 °C for 3 h, neutralized with aq.  $\text{KHSO}_4$ , and purified via column chromatography ( $\text{SiO}_2$ , eluent: methanol/dichloromethane, 1:9,  $v/v$ ). White solid; yield 79% (251 mg); m.p. 220–221 °C.  $^1\text{H}$  NMR (700 MHz, DMSO- $d_6$ ):  $\delta_{\text{H}}$  ppm 3.77 (s, 3H,  $\text{CH}_3$ ), 7.45 (t,  $J = 7.4$  Hz, 1H, NPh 4-H), 7.56–7.61 (m, 5H, NPh 3,5-H and 6-CPh 3,4,5-H), 7.96–7.98 (m, 2H, 6-CPh 2,6-H), 8.00 (d,  $J = 8.0$  Hz, 2H, NPh 2,6-H), 9.34 (s, 1H, 3-H).  $^{13}\text{C}$  NMR (176 MHz, DMSO- $d_6$ ):  $\delta_{\text{C}}$  ppm 60.1 ( $\text{CH}_3$ ), 109.8 (C-3a), 119.5 (NPh C-2,6), 126.5 (C-3), 128.1 (NPh C-4), 128.2 (6-CPh C-2,6), 128.7 (6-CPh C-3,5), 129.8 (NPh C-3,5), 130.4 (6-CPh C-1), 130.7 (6-CPh C-4), 138.7 (NPh C-1), 140.8 (C-5), 154.1 (C-6), 160.8 (C-7a), 172.1 (C-4).  $^{15}\text{N}$  NMR (71 MHz, DMSO- $d_6$ ):  $\delta_{\text{N}}$  ppm –168.0 (N-2), –115.9 (N-1). IR ( $\nu_{\text{max}}$ ,  $\text{cm}^{-1}$ ): 3101, 2936, 1640 (C=O), 1578, 1554, 1443, 1351, 1134, 764, 753, 682. HRMS (ESI $^+$ ) for  $\text{C}_{19}\text{H}_{14}\text{N}_2\text{NaO}_3$  ( $[\text{M} + \text{Na}]^+$ ) calcd 341.0897, found 341.0899.

### 3.2.4. Procedure for the Synthesis of 6-(1-Methylpyridin-1-ium-4-yl)-4-oxo-2-phenyl-2,4-dihydropyrano[2,3-c]pyrazol-5-olate (5)

To a solution of **3a** (304 mg, 1 mmol) in dioxane (30 mL),  $\text{Cs}_2\text{CO}_3$  (0.65 g, 2 mmol) and MeI (0.07 mL, 1.1 mmol) were added. The reaction mixture was stirred at 40 °C for 3 h, neutralized with aq.  $\text{KHSO}_4$ , and purified via column chromatography ( $\text{SiO}_2$ , eluent: methanol/dichloromethane, 1:9,  $v/v$ ). Red solid; yield 59% (264 mg); decomposition 240–241 °C.  $^1\text{H}$  NMR (700 MHz, DMSO- $d_6$ )  $\delta$  3.95 ( $\text{CH}_3$ ), 7.42 (m, 1H, Ph 4-H), 7.56 (m, 2H,

Ph 3,5-H), 7.98 (m, 2H, Ph 2,6-H), 8.12–8.20 (m, 2H, Pyr 2,6-H), 9.14–9.20 (m, 2H, Pyr 3,5-H), 9.41 (s, 1H, 3-H).  $^{13}\text{C}$  NMR (176 MHz, DMSO- $d_6$ )  $\delta$  44.5 (CH<sub>3</sub>), 109.4 (C-3a), 112.9 (Pyr C-5), 114.6 (Pyr C-3), 119.1 (Ph C-2,6), 126.7 (C-3), 127.6 (Ph C-4), 129.6 (Ph C-3,5), 134.8 (C-6), 138.7 (Ph C-1), 140.9 (Pyr C-6), 141.6 (Pyr C-2), 143.3 (Pyr C-4), 161.2 (C-7a), 164.1 (C-5), 176.1 (C-4).  $^{15}\text{N}$  NMR (71 MHz, DMSO- $d_6$ ):  $\delta_{\text{N}}$  ppm –214.4 (Pyr N); –170.1 (N-2), –120.2 (N-1). IR ( $\nu_{\text{max}}$ ,  $\text{cm}^{-1}$ ): 3089, 2920, 2852, 1629 (C=O), 1569, 1488, 1465, 1382, 1189, 756, 689. HRMS (ESI<sup>+</sup>) for C<sub>18</sub>H<sub>14</sub>N<sub>3</sub>O<sub>3</sub> ([M + Na]<sup>+</sup>) calcd 342.0849, found 342.0852.

### 3.2.5. Procedure for the Synthesis of 4-(5-Hydroxy-4-oxo-2-phenyl-2,4-dihydropyrano pyrazol-6-yl)-1-methylpyridin-1-ium Iodide (6)

To a solution of **3a** (305 mg, 1 mmol) in ACN (15 mL), MeI (1 mL, 16.1 mmol) was added. The reaction mixture was stirred at 40 °C for 2 h and diluted with DMF (15 mL); the solution was slowly dripped into cold diethyl ether. The formed crystals were filtrated and washed with a small amount of MeOH and diethyl ether. Orange solid; yield 78% (348 mg); decomposition 277–278 °C.  $^1\text{H}$  NMR (700 MHz, DMSO- $d_6$ )  $\delta$  4.39 (CH<sub>3</sub>), 7.47 (m, 1H, Ph 4-H), 7.58 (m, 2H, Ph 3,5-H), 7.97 (m, 2H, Ph 2,6-H), 8.63 (m, 2H, Pyr 3,5-H), 9.03 (m, 2H, Pyr 2,6-H), 9.45 (s, 1H, 3-H), 11.49 (s, 1H, OH).  $^{13}\text{C}$  NMR (176 MHz, DMSO- $d_6$ )  $\delta$  48.0 (CH<sub>3</sub>), 108.4 (C-3a), 119.9 (Ph C-2,6), 123.8 (Pyr C-3,5), 127.4 (C-3), 128.9 (Ph C-4), 130.3 (Ph C-3,5), 146.1 (Pyr C-4), 138.8 (Ph C-1), 137.5 (C-6), 145.4 (C-5), 145.9 (Pyr C-2,6), 160.7 (C-7a), 171.4 (C-4).  $^{15}\text{N}$  NMR (71 MHz, DMSO- $d_6$ ):  $\delta_{\text{N}}$  ppm –183.2 (Pyr N); –165.7 (N-2), –117.1 (N-1). IR ( $\nu_{\text{max}}$ ,  $\text{cm}^{-1}$ ): 3135, 3066, 1646 (C=O), 1575, 1497, 1441, 1388, 1232, 1197, 1109, 761. HRMS (ESI<sup>+</sup>) for C<sub>18</sub>H<sub>14</sub>N<sub>3</sub>O<sub>3</sub> (M<sup>+</sup>) calcd 320.1030, found 320.1032.

### 3.2.6. Procedure for the Synthesis of 4-Oxo-2,6-diphenyl-2,4-dihydropyrano[2,3-*c*]pyrazol-5-yl Trifluoromethanesulfonate (7)

To a solution of **3a** (304 mg, 1 mmol) in DCM (30 mL), at 0 °C, TEA (0.7 mL, 5 mmol) and Tf<sub>2</sub>O (0.34 mL, 2 mmol) were added dropwise. The reaction mixture was stirred at 24 °C for 16 h, diluted with DCM (100 mL), washed with brine (100 mL), and purified via column chromatography (SiO<sub>2</sub>, eluent: ethyl acetate/*n*-hexane, 1:6, *v/v*). Beige solid; yield 74% (323 mg); m.p. 200–201 °C.  $^1\text{H}$  NMR (700 MHz, CDCl<sub>3</sub>):  $\delta_{\text{H}}$  ppm 7.46 (t, *J* = 7.3 Hz, 1H, NPh 4-H), 7.55–7.58 (m, 4H, NPh 3,5-H and 6-CPh 3,5-H), 7.62 (t, *J* = 7.3 Hz, 1H, 6-CPh 4-H), 7.78 (d, *J* = 8.0 Hz, 2H, NPh 2,6-H), 7.87 (d, *J* = 7.5 Hz, 2H, 6-CPh 2,6-H), 8.59 (s, 1H, 3-H).  $^{13}\text{C}$  NMR (176 MHz, CDCl<sub>3</sub>):  $\delta_{\text{C}}$  ppm 109.4 (C-3a), 118.2 (q,  $^1J_{\text{C,F}}$  = 320.8 Hz, CF<sub>3</sub>), 120.3 (NPh C-2,6), 125.5 (C-3), 128.4 (6-CPh C-1), 129.0 (6-CPh C-3,5), 129.1 (NPh C-4), 129.2 (6-CPh C-2,6), 130.1 (NPh C-3,5), 132.6 (6-CPh C-4), 134.6 (C-5), 138.9 (NPh C-1), 158.2 (C-6), 161.3 (C-7a), 168.8 (C-4).  $^{15}\text{N}$  NMR (71 MHz, CDCl<sub>3</sub>):  $\delta_{\text{N}}$  ppm –165.8 (N-2), –112.7 (N-1).  $^{19}\text{F}$  NMR (376 MHz, CDCl<sub>3</sub>):  $\delta_{\text{F}}$  ppm –74.0 (CF<sub>3</sub>). IR ( $\nu_{\text{max}}$ ,  $\text{cm}^{-1}$ ): 3105, 2918, 1658 (C=O), 1594, 1553, 1425, 1208, 1134, 1019, 897, 757, 686, 600. HRMS (ESI<sup>+</sup>) for C<sub>19</sub>H<sub>11</sub>F<sub>3</sub>N<sub>2</sub>NaO<sub>5</sub>S ([M + Na]<sup>+</sup>) calcd 459.0233, found 459.0235.

### 3.2.7. General Procedure for the Synthesis of 5-(Hetero)aryl-2,6-diphenylpyrano[2,3-*c*]pyrazol-4(2*H*)-ones **8a–e**

To a solution of **7** (436 mg, 1 mmol) in dioxane (15 mL), K<sub>3</sub>PO<sub>4</sub> (634 mg, 3 mmol), KBr (131 mg, 1.1 mmol), appropriate (hetero)arylboronic acid (2.5 mmol), and Pd(PPh<sub>3</sub>)<sub>4</sub> (69 mg, 0.06 mmol) were added. The reaction mixture was stirred at 90 °C for 16 h, diluted with H<sub>2</sub>O (80 mL), extracted with DCM (3 × 15 mL), and purified via column chromatography (SiO<sub>2</sub>, eluent: ethyl acetate/*n*-hexane, 1:6, *v/v*).

**2,5,6-Triphenylpyrano[2,3-*c*]pyrazol-4(2*H*)-one (8a)**. Yellow solid; yield 95% (346 mg); m.p. 265–266 °C.  $^1\text{H}$  NMR (700 MHz, CDCl<sub>3</sub>):  $\delta_{\text{H}}$  ppm 7.20–7.21 (m, 2H, 5-CPh 2,6-H), 7.24–7.25 (m, 2H, 6-CPh 3,5-H), 7.28–7.33 (m, 4H, 5-CPh 3,4,5-H and 6-CPh 4-H), 7.39 (d, *J* = 7.6 Hz, 2H, 6-CPh 2,6-H), 7.42 (t, *J* = 7.4 Hz, 1H, NPh 4-H), 7.53 (t, *J* = 7.9 Hz, 2H, NPh 3,5-H), 7.80 (d, *J* = 8.0 Hz, 2H, NPh 2,6-H), 8.55 (s, 1H, 3-H).  $^{13}\text{C}$  NMR (176 MHz, CDCl<sub>3</sub>):  $\delta_{\text{C}}$  ppm 109.7 (C-3a), 119.9 (NPh C-2,6), 123.0 (C-5), 124.7 (C-3), 127.7 (5-CPh C-4), 128.0 (6-CPh C-3,5), 128.24 (NPh C-4), 128.29 (5-CPh C-3,5), 129.78 (6-CPh C-2,6), 129.83 (NPh C-3,5),

130.0 (6-CPh C-4), 131.4 (5-CPh C-2,6), 132.8 (5-CPh C-1), 133.0 (6-CPh C-1), 139.2 (NPh C-1), 160.8 (C-6), 162.4 (C-7a), 175.5 (C-4).  $^{15}\text{N}$  NMR (71 MHz,  $\text{CDCl}_3$ ):  $\delta_{\text{N}}$  ppm  $-169.5$  (N-2),  $-115.3$  (N-1). IR ( $\nu_{\text{max}}$ ,  $\text{cm}^{-1}$ ): 3093, 2922, 1642 (C=O), 1578, 1561, 1493, 1349, 1224, 1056, 755, 730, 694, 683. HRMS (ESI $^{+}$ ) for  $\text{C}_{24}\text{H}_{16}\text{N}_2\text{NaO}_2$  ( $[\text{M} + \text{Na}]^{+}$ ) calcd 387.1104, found 387.1107.

*5-(4-Methylphenyl)-2,6-diphenylpyrano[2,3-*c*]pyrazol-4(2H)-one (8b)*. White solid; yield 62% (235 mg); m.p. 256–257 °C.  $^1\text{H}$  NMR (700 MHz,  $\text{CDCl}_3$ ):  $\delta_{\text{H}}$  ppm 2.34 (s, 3H,  $\text{CH}_3$ ), 7.08 (m, 2H, 5-CPh 2,6-H), 7.11 (m, 2H, 5-CPh 3,5-H), 7.24–7.27 (m, 2H, 6-CPh 3,5-H), 7.32 (m, 2H, 6-CPh 4-H), 7.40–7.43 (m, 3H, 6-CPh 2,6-H, NPh 4-H), 7.53 (m, 2H, NPh 3,5-H), 7.78–7.81 (m, 2H, NPh 2,6-H), 8.55 (s, 1H, 3-H).  $^{13}\text{C}$  NMR (176 MHz,  $\text{CDCl}_3$ ):  $\delta_{\text{C}}$  ppm 21.3 ( $\text{CH}_3$ ), 109.7 (C-3a), 119.8 (NPh C-2,6), 122.9 (C-5), 124.6 (C-3), 128.0 (6-CPh C-3,5), 128.2 (NPh C-4), 129.1 (5-CPh C-3,5), 129.6 (5-CPh C-1), 129.7 (6-CPh C-2,6), 129.8 (NPh C-3,5), 129.9 (6-Ph C-4), 131.2 (5-CPh C-2,6), 133.1 (6-CPh C-1), 137.4 (5-CPh C-4), 139.2 (NPh C-1), 160.5 (C-6), 162.3 (C-7a), 175.7 (C-4).  $^{15}\text{N}$  NMR (71 MHz,  $\text{CDCl}_3$ ):  $\delta_{\text{N}}$  ppm  $-169.7$  (N-2),  $-115.3$  (N-1). IR ( $\nu_{\text{max}}$ ,  $\text{cm}^{-1}$ ): 3098, 3023, 1649 (C=O), 1578, 1565, 1348, 1181, 1021, 755, 742, 732, 683. HRMS (ESI $^{+}$ ) for  $\text{C}_{25}\text{H}_{18}\text{N}_2\text{O}_2$  ( $[\text{M} + \text{Na}]^{+}$ ) calcd 401.1260, found 401.1262.

*5-(4-Methoxyphenyl)-2,6-diphenylpyrano[2,3-*c*]pyrazol-4(2H)-one (8c)*. White solid; yield 77% (304 mg); m.p. 236–237 °C.  $^1\text{H}$  NMR (700 MHz,  $\text{CDCl}_3$ ):  $\delta_{\text{H}}$  ppm 3.80 (s, 3H,  $\text{CH}_3$ ), 6.85 (m, 2H, 5-CPh 3,5-H), 7.12 (m, 2H, 5-CPh 2,6-H), 7.24–7.28 (m, 2H, 6-CPh 3,5-H), 7.32 (m, 2H, 6-CPh 4-H), 7.40–7.44 (m, 3H, 6-CPh 2,6-H, NPh 4-H), 7.54 (m, 2H, NPh 3,5-H), 7.80 (m, 2H, NPh 2,6-H), 8.54 (s, 1H, 3-H).  $^{13}\text{C}$  NMR (176 MHz,  $\text{CDCl}_3$ ):  $\delta_{\text{C}}$  ppm 55.2 ( $\text{CH}_3$ ), 109.7 (C-3a), 113.9 (5-CPh C-3,5), 119.8 (NPh C-2,6), 122.5 (C-5), 124.6 (C-3), 124.8 (5-CPh C-1), 128.0 (6-CPh C-3,5), 128.2 (NPh C-4), 129.7 (6-CPh C-2,6), 129.8 (NPh C-3,5), 129.9 (6-Ph C-4), 132.5 (5-CPh C-2,6), 133.2 (6-CPh C-1), 139.2 (NPh C-1), 159.1 (5-CPh C-4), 160.5 (C-6), 162.3 (C-7a), 175.8 (C-4).  $^{15}\text{N}$  NMR (71 MHz,  $\text{CDCl}_3$ ):  $\delta_{\text{N}}$  ppm  $-169.7$  (N-2),  $-115.6$  (N-1). IR ( $\nu_{\text{max}}$ ,  $\text{cm}^{-1}$ ): 3102, 3024, 1650 (C=O), 1598, 1567, 1335, 1241, 1167, 1023, 748, 686, 549. HRMS (ESI $^{+}$ ) for  $\text{C}_{25}\text{H}_{18}\text{N}_2\text{O}_3$  ( $[\text{M} + \text{Na}]^{+}$ ) calcd 417.1210, found 417.1208.

*5-(4-Chlorophenyl)-2,6-diphenylpyrano[2,3-*c*]pyrazol-4(2H)-one (8d)*. White solid; yield 44% (176 mg); m.p. 255–256 °C.  $^1\text{H}$  NMR (700 MHz,  $\text{CDCl}_3$ ):  $\delta_{\text{H}}$  ppm 7.14 (m, 2H, 5-CPh 2,6-H), 7.27–7.31 (m, 4H, 5-CPh 3,5-H, 6-CPh 3,5-H), 7.35 (m, 2H, 6-CPh 4-H), 7.39 (m, 2H, 6-CPh 2,6-H), 7.43 (m, 1H, NPh 4-H), 7.54 (m, 2H, NPh 3,5-H), 7.80 (m, 2H, NPh 2,6-H), 8.55 (s, 1H, 3-H).  $^{13}\text{C}$  NMR (176 MHz,  $\text{CDCl}_3$ ):  $\delta_{\text{C}}$  ppm 109.5 (C-3a), 119.9 (NPh C-2,6), 121.8 (C-5), 124.7 (C-3), 128.2 (6-CPh C-3,5), 128.4 (NPh C-4), 128.6 (5-CPh C-3,5), 129.7 (6-CPh C-2,6), 129.8 (NPh C-3,5), 130.3 (6-Ph C-4), 131.3 (5-CPh C-1), 132.7 (6-CPh C-1), 132.8 (5-CPh C-2,6), 133.7 (5-CPh C-4), 139.1 (NPh C-1), 161.0 (C-6), 162.32 (C-7a), 175.2 (C-4).  $^{15}\text{N}$  NMR (71 MHz,  $\text{CDCl}_3$ ):  $\delta_{\text{N}}$  ppm  $-169.1$  (N-2),  $-115.0$  (N-1). IR ( $\nu_{\text{max}}$ ,  $\text{cm}^{-1}$ ): 3206, 3105, 1650 (C=O), 1568, 1422, 1348, 1211, 1135, 757, 731, 686. HRMS (ESI $^{+}$ ) for  $\text{C}_{24}\text{H}_{15}\text{ClN}_2\text{O}_2$  ( $[\text{M} + \text{Na}]^{+}$ ) calcd 421.0714, found 421.0711.

*2,6-Diphenyl-5-(thiophen-3-yl)pyrano[2,3-*c*]pyrazol-4(2H)-one (8e)*. Beige solid; yield 80% (297 mg); m.p. 265–266 °C.  $^1\text{H}$  NMR (700 MHz,  $\text{CDCl}_3$ ):  $\delta_{\text{H}}$  ppm 6.88 (m, 1H, Th 4-H), 7.20 (m, 1H, Th 2-H), 7.24 (m, 1H, Th 5-H), 7.31 (m, 2H, 6-CPh 3,5-H), 7.37 (m, 2H, 6-CPh 4-H), 7.42 (m, 1H, NPh 4-H), 7.44 (m, 2H, 6-CPh 2,6-H), 7.54 (m, 2H, NPh 3,5-H), 7.80 (m, 2H, NPh 2,6-H), 8.54 (s, 1H, 3-H).  $^{13}\text{C}$  NMR (176 MHz,  $\text{CDCl}_3$ ):  $\delta_{\text{C}}$  ppm 109.6 (C-3a), 118.1 (C-5), 119.9 (NPh C-2,6), 124.6 (C-3), 124.7 (Th C-5), 126.4 (Th C-2), 128.1 (6-CPh C-3,5), 128.3 (NPh C-4), 129.8 (Th C-4), 129.5 (6-CPh C-2,6), 129.8 (NPh C-3,5), 130.2 (6-Ph C-4), 131.9 (Th C-3), 132.2 (6-CPh C-1), 139.1 (NPh C-1), 160.8 (C-6), 162.2 (C-7a), 175.3 (C-4).  $^{15}\text{N}$  NMR (71 MHz,  $\text{CDCl}_3$ ):  $\delta_{\text{N}}$  ppm  $-169.4$  (N-2),  $-115.2$  (N-1). IR ( $\nu_{\text{max}}$ ,  $\text{cm}^{-1}$ ): 3100, 1644 (C=O), 1577, 1564, 1441, 1328, 1218, 753, 739, 685. HRMS (ESI $^{+}$ ) for  $\text{C}_{22}\text{H}_{14}\text{N}_2\text{O}_2\text{S}$  ( $[\text{M} + \text{H}]^{+}$ ) calcd 393.0668, found 393.0669.

### 3.2.8. Procedure for the Synthesis of *tert*-Butyl (2*E*)-3-(4-oxo-2,6-diphenyl-2,4-dihydropyrano[2,3-*c*]pyrazol-5-yl)prop-2-enoate (**8f**)

To a solution of **7** (436 mg, 1 mmol) in dry DMF (10 mL), TEA (0.28 mL, 2 mmol), *tert*-butyl acrylate (0.29 mL, 2 mmol), and Pd(PPh<sub>3</sub>)<sub>2</sub>Cl<sub>2</sub> (35 mg, 0.05 mmol) were added. The reaction mixture was stirred at 100 °C for 72 h, diluted with H<sub>2</sub>O (100 mL), extracted with EtOAc (3 × 50 mL), washed with brine (100 mL), and purified via column chromatography (SiO<sub>2</sub>, eluent: dichloromethane). White solid; yield 24% (99 mg); decomposition 312 °C. <sup>1</sup>H NMR (700 MHz, CDCl<sub>3</sub>): δ<sub>H</sub> ppm 1.48 (s, 9H, C(CH<sub>3</sub>)<sub>3</sub>), 7.31 (d, *J* = 15.9 Hz, 1H, CHCHCOOC(CH<sub>3</sub>)<sub>3</sub>), 7.35 (d, *J* = 15.8 Hz, 1H, CHCHCOOC(CH<sub>3</sub>)<sub>3</sub>), 7.42 (t, *J* = 7.4 Hz, 1H, NPh 4-H), 7.52–7.56 (m, 5H, NPh 3,5-H and 6-CPh 3,4,5-H), 7.68 (d, *J* = 6.8 Hz, 2H, 6-CPh 2,6-H), 7.79 (d, *J* = 8.0 Hz, 2H, NPh 2,6-H), 8.54 (s, 1H, 3-H). <sup>13</sup>C NMR (176 MHz, CDCl<sub>3</sub>): δ<sub>C</sub> ppm 28.2 (C(CH<sub>3</sub>)<sub>3</sub>), 80.3 (C(CH<sub>3</sub>)<sub>3</sub>), 110.0 (C-3a), 115.9 (C-5), 120.0 (NPh C-2,6), 125.0 (C-5), 125.5 (CHCHCOOC(CH<sub>3</sub>)<sub>3</sub>), 128.6 (NPh C-4), 128.8 (6-CPh C-3,5), 130.0 (NPh C-3,5), 130.2 (6-CPh C-2,6), 131.6 (6-CPh C-4), 132.1 (6-CPh C-1), 135.3 (CHCHCOOC(CH<sub>3</sub>)<sub>3</sub>), 139.2 (NPh C-1), 161.7 (C-7a), 166.0 (C-6), 167.1 (CHCHCOOC(CH<sub>3</sub>)<sub>3</sub>), 175.2 (C-4). <sup>15</sup>N NMR (71 MHz, CDCl<sub>3</sub>): δ<sub>N</sub> ppm –168.8 (N-2), –114.4 (N-1). IR (ν<sub>max</sub>, cm<sup>–1</sup>): 3106, 2971, 1647 (C=O), 1584, 1554, 1445, 1290, 1149, 753, 688. HRMS (ESI<sup>+</sup>) for C<sub>25</sub>H<sub>22</sub>N<sub>2</sub>NaO<sub>4</sub> ([M + Na]<sup>+</sup>) calcd 437.1472, found 437.1473.

### 3.2.9. Procedure for the Synthesis of 2,6-Diphenyl-5-(phenylethynyl)pyrano[2,3-*c*]pyrazol-4(2*H*)-one (**8g**)

To a solution of **7** (436 mg, 1 mmol) in dry DMF (10 mL), TEA (0.28 mL, 2 mmol), CuI (19 mg, 0.1 mmol), phenylacetylene (0.16 mL, 1.5 mmol), and Pd(PPh<sub>3</sub>)<sub>2</sub>Cl<sub>2</sub> (42 mg, 0.06 mmol) were added. The reaction mixture was stirred at 65 °C for 1 h, diluted with H<sub>2</sub>O (100 mL), extracted with EtOAc (3 × 50 mL), washed with brine (100 mL), and purified via column chromatography, (SiO<sub>2</sub>, eluent: dichloromethane). White solid; yield 71% (276 mg); m.p. 222–223 °C. <sup>1</sup>H NMR (700 MHz, CDCl<sub>3</sub>): δ<sub>H</sub> ppm 7.31–7.34 (m, 3H, C≡CPh 3,4,5-H), 7.42 (t, *J* = 7.4 Hz, 1H, NPh 4-H), 7.49–7.50 (m, 2H, C≡CPh 2,6-H), 7.52–7.57 (m, 5H, NPh 3,5-H and 6-CPh 3,4,5-H), 7.79 (d, *J* = 8.1 Hz, 2H, NPh 2,6-H), 8.25 (d, *J* = 7.9 Hz, 2H, 6-CPh 2,6-H), 8.55 (s, 1H, 3-H). <sup>13</sup>C NMR (176 MHz, CDCl<sub>3</sub>): δ<sub>C</sub> ppm 82.0 (C≡CPh), 97.9 (C≡CPh), 107.7 (C-5), 108.8 (C-3a), 120.0 (NPh C-2,6), 123.3 (C≡CPh C-1), 124.8 (C-3), 128.3 (6-CPh C-3,5), 128.4 (C≡CPh C-3,5), 128.6 (C≡CPh C-4 and NPh C-4), 129.4 (6-CPh C-2,6), 130.0 (NPh C-3,5), 131.66 (6-CPh C-4), 131.71 (C≡CPh C-2,6), 132.3 (6-CPh C-1), 139.1 (NPh C-1), 161.9 (C-7a), 165.1 (C-6), 174.2 (C-4). <sup>15</sup>N NMR (71 MHz, CDCl<sub>3</sub>): δ<sub>N</sub> ppm –168.6 (N-2), –114.3 (N-1). IR (ν<sub>max</sub>, cm<sup>–1</sup>): 3094, 3057, 1649 (C=O), 1577, 1542, 1442, 1361, 1264, 1118, 750, 684. HRMS (ESI<sup>+</sup>) for C<sub>26</sub>H<sub>16</sub>N<sub>2</sub>NaO<sub>2</sub> ([M + Na]<sup>+</sup>) calcd 411.1104, found 411.1101.

## 4. Conclusions

In conclusion, we showed that the diverse 6-aryl-5-hydroxy-2-phenylpyrano[2,3-*c*]pyrazol-4(2*H*)-one derivatives as analogues of 3-hydroxyflavones can be conveniently synthesized from appropriate (*E*)-1-(3-hydroxy-1-phenyl-1*H*-pyrazol-4-yl)prop-2-en-1-ones employing Algar–Flynn–Oyamada reaction conditions. Further functionalization of the 5-position of the pyrano[2,3-*c*]pyrazol-4(2*H*)-one ring was achieved by employing various Pd-catalyzed coupling reactions of the intermediate 5-triflate. Extensive NMR spectroscopic studies were undertaken using standard and advanced methods to unambiguously determine the structure and configuration of the synthesized compounds. The synthesized 3-hydroxyflavone analogues were characterized by good quantum yields and large Stokes shifts. In addition, the excited-state intramolecular proton transfer (ESIPT) reaction of 5-hydroxypyrano[2,3-*c*]pyrazol-4(2*H*)-one from the 5-hydroxy moiety to the carbonyl group in polar protic, polar aprotic, and non-polar solvents was observed, resulting in a well-resolved two-band fluorescence.

**Supplementary Materials:** The following supporting information can be downloaded at: <https://www.mdpi.com/article/10.3390/molecules28186599/s1>. Table S1: Optimization of AFO reaction conditions of (*E*)-1-(3-hydroxy-1-phenyl-1*H*-pyrazol-4-yl)-3-phenylprop-2-en-1-one (**2a**) to get 5-hydroxy-2,6-diphenylpyrano[2,3-*c*]pyrazol-4(2*H*)-one (**3a**); Table S2: Relevant <sup>1</sup>H and <sup>13</sup>C NMR spectral data of 6-(hetero)aryl-5-hydroxy-2-phenylpyrano[2,3-*c*]pyrazol-4(2*H*)-ones **3a–h** in DMSO-*d*<sub>6</sub> (δ in ppm); Tables S3–S11: Data for X-ray analysis of compound **5**; Table S3: Experimental parameters and CCDC-2287991; Table S4: Sample and crystal data of compound **5**; Table S5: Data collection and structure refinement of compound **5**; Table S6: Methanol formed and other selected hydrogen bonds in monocystal of compound **5**; Table S7: Fractional Atomic Coordinates (×10<sup>4</sup>) and Equivalent Isotropic Displacement Parameters (Å<sup>2</sup> × 10<sup>3</sup>) for compound **5**; Table S8: Anisotropic displacement parameters (Å<sup>2</sup> × 10<sup>3</sup>) for compound **5**; Table S9: Bond lengths for compound **5**; Table S10: Bond angles for compound **5**; Table S11: Hydrogen atom coordinates (Å × 10<sup>4</sup>) and isotropic displacement parameters (Å<sup>2</sup> × 10<sup>3</sup>) for compound **5**; Figure S1: (a) UV absorption spectra of compounds **4** and **8a,f,g** in THF; (b) fluorescence emission spectra (λ<sub>ex</sub> = 340 nm) of compounds **4** and **8a,f,g** in THF; Table S12: Absorption (λ<sub>abs</sub> absorption maxima and ε), fluorescence emission (λ<sub>em</sub> and quantum yield Φ<sub>f</sub>), and Stokes shift parameters for **4** and **8a,f,g** in THF (\*λ<sub>ex</sub> = 340 nm); Figures S2–S81: <sup>1</sup>H, <sup>13</sup>C, <sup>1</sup>H-<sup>15</sup>N HMBC NMR, and HRMS (ESI) spectra of compounds **2d**, **3a–h**, **4–7**, **8a–g**. References [80–82] are cited in the Supplementary Materials.

**Author Contributions:** Conceptualization, A.Š.; methodology, A.Š., E.A. and S.K.; formal analysis, A.Š. and E.A.; investigation, A.U. and A.B.; resources, A.Š. and E.A.; data curation, A.Š., A.U., A.B. and E.A.; writing—original draft preparation, A.Š., E.A., A.B., V.M. and A.U.; writing—review and editing, A.Ž. and J.S.; visualization, A.Š. and A.U.; supervision, S.K., E.A. and A.Š.; funding acquisition, A.Š. and E.A. All authors have read and agreed to the published version of the manuscript.

**Funding:** This research was funded by the Research Council of Lithuania (No. S-MIP-23-51).

**Institutional Review Board Statement:** Not applicable.

**Informed Consent Statement:** Not applicable.

**Data Availability Statement:** The data that support the findings of this study are available from the corresponding author upon reasonable request.

**Acknowledgments:** The authors are grateful to S. Belyakov (Latvian Institute of Organic Synthesis, Riga, Latvia) for performing the X-ray analysis.

**Conflicts of Interest:** The authors declare no conflict of interest.

**Sample Availability:** Not available.

## References

1. Li, M.-M.; Huang, H.; Pu, Y.; Tian, W.; Deng, Y.; Lu, J. A close look into the biological and synthetic aspects of fused pyrazole derivatives. *Eur. J. Med. Chem.* **2022**, *243*, 114739. [[CrossRef](#)] [[PubMed](#)]
2. Hassan, A.Y.; Mohamed, M.A.; Abdel-Aziem, A.; Hussain, A.O. Synthesis and Anticancer Activity of Some Fused Heterocyclic Compounds Containing Pyrazole Ring. *Polycycl. Aromat. Compd.* **2020**, *40*, 1280–1290. [[CrossRef](#)]
3. Bondock, S.; Fadaly, W.; Metwally, M.A. Synthesis and antimicrobial activity of some new thiazole, thiophene and pyrazole derivatives containing benzothiazole moiety. *Eur. J. Med. Chem.* **2010**, *45*, 3692–3701. [[CrossRef](#)]
4. Han, C.; Guo, Y.-C.; Wang, D.-D.; Dai, X.-Y.; Wu, F.-J.; Liu, H.-F.; Dai, G.-F.; Tao, J.-C. Novel pyrazole fused heterocyclic ligands: Synthesis, characterization, DNA binding/cleavage activity and anti-BVDV activity. *Chin. Chem. Lett.* **2015**, *26*, 534–538. [[CrossRef](#)]
5. Pinto, D.J.P.; Orwat, M.J.; Koch, S.; Rossi, K.A.; Alexander, R.S.; Smallwood, A.; Wong, P.C.; Rendina, A.R.; Luetzgen, J.M.; Knabb, R.M.; et al. Discovery of 1-(4-Methoxyphenyl)-7-oxo-6-(4-(2-oxopiperidin-1-yl)phenyl)-4,5,6,7-tetrahydro-1*H*-pyrazolo[3,4-*c*]pyridine-3-carboxamide (Apixaban, BMS-562247), a Highly Potent, Selective, Efficacious, and Orally Bioavailable Inhibitor of Blood Coagulation Factor Xa. *J. Med. Chem.* **2007**, *50*, 5339–5356. [[PubMed](#)]
6. Xu, Y.; Zhang, Z.; Jiang, X.; Chen, X.; Wang, Z.; Alsulami, H.; Qin, H.-L.; Tang, W. Discovery of δ-sultone-fused pyrazoles for treating Alzheimer's disease: Design, synthesis, biological evaluation and SAR studies. *Eur. J. Med. Chem.* **2019**, *181*, 111598. [[CrossRef](#)]
7. Syed, Y.Y. Futibatinib: First Approval. *Drugs* **2022**, *82*, 1737–1743. [[CrossRef](#)]
8. Kumar, A.; Lohan, P.; Aneja, D.K.; Gupta, G.K.; Kaushik, D.; Prakash, O. Design, synthesis, computational and biological evaluation of some new hydrazino derivatives of DHA and pyranopyrazoles. *Eur. J. Med. Chem.* **2012**, *50*, 81–89. [[CrossRef](#)]

9. Parikh, P.H.; Timaniya, J.B.; Patel, M.J.; Patel, K.P. Microwave-assisted synthesis of pyrano[2,3-*c*]-pyrazole derivatives and their anti-microbial, anti-malarial, anti-tubercular, and anti-cancer activities. *J. Mol. Struct.* **2022**, *1249*, 131605. [[CrossRef](#)]
10. Parshad, M.; Verma, V.; Kumar, D. Iodine-mediated efficient synthesis of pyrano[2,3-*c*]pyrazoles and their antimicrobial activity. *Monatsh. Chem.* **2014**, *145*, 1857–1865. [[CrossRef](#)]
11. Wang, J.; Liu, D.; Zheng, Z.; Shan, S.; Han, X.; Srinivasula, S.M.; Croce, C.M.; Alnemri, E.S.; Huang, Z. Structure-based discovery of an organic compound that binds Bcl-2 protein and induces apoptosis of tumor cells. *Proc. Natl. Acad. Sci. USA* **2000**, *97*, 7124–7129. [[CrossRef](#)] [[PubMed](#)]
12. Sun, X.; Zhang, L.; Gao, M.; Que, X.; Zhou, C.; Zhu, D.; Cai, Y. Nanof ormulation of a Novel Pyrano[2,3-*c*]Pyrazole Heterocyclic Compound AMDPC Exhibits Anti-Cancer Activity via Blocking the Cell Cycle through a P53-Independent Pathway. *Molecules* **2019**, *24*, 624. [[CrossRef](#)] [[PubMed](#)]
13. Nguyen, H.T.; Truong, M.-N.H.; Le, T.V.; Vo, N.T.; Nguyen, H.D.; Tran, P.H. A New Pathway for the Preparation of Pyrano[2,3-*c*]pyrazoles and molecular Docking as Inhibitors of p38 MAP Kinase. *ACS Omega* **2022**, *7*, 17432–17443. [[CrossRef](#)] [[PubMed](#)]
14. Bieliauskas, A.; Krikštolaitytė, S.; Holzer, W.; Šačkus, A. Ring-closing metathesis as a key step to construct 2,6-dihydropyrano[2,3-*c*]pyrazole ring system. *Arkivoc* **2018**, *2018*, 296–307. [[CrossRef](#)]
15. Milišūnaitė, V.; Kadlecová, A.; Žukauskaitė, A.; Doležal, K.; Strnad, M.; Voller, J.; Arbačiauskienė, E.; Holzer, W.; Šačkus, A. Synthesis and Anthelmintic Activity of Benzopyrano[2,3-*c*]Pyrazol-4(2*H*)-One Derivatives. *Mol. Divers.* **2020**, *24*, 1025–1042. [[CrossRef](#)]
16. Al-Khayri, J.M.; Sahana, G.R.; Nagella, P.; Joseph, B.V.; Alessa, F.M.; Al-Mssallem, M.Q. Flavonoids as Potential Anti-Inflammatory. *Molecules* **2022**, *27*, 2901. [[CrossRef](#)]
17. Panche, A.; Diwan, A.; Chandra, S. Flavonoids: An overview. *J. Nutr. Sci.* **2016**, *5*, E47. [[CrossRef](#)]
18. Ullah, A.; Munir, S.; Badshah, S.L.; Khan, N.; Ghani, L.; Poulson, B.G.; Mews, A.-H.; Jaremko, M. Important Flavonoids and Their Role as a Therapeutic Agent. *Molecules* **2020**, *25*, 5243. [[CrossRef](#)]
19. Jan, R.; Khan, M.; Asaf, S.; Lubna; Asif, S.; Kim, K.-M. Bioactivity and Therapeutic Potential of Kaempferol and Quercetin: New Insights for Plant and Human Health. *Plants* **2022**, *11*, 2623. [[CrossRef](#)]
20. Nejabati, H.R.; Roshangar, L. Kaempferol: A potential agent in the prevention of colorectal cancer. *Physiol. Rep.* **2022**, *10*, e15488. [[CrossRef](#)]
21. Borsari, C.; Jiménez-Antón, M.D.; Eick, J.; Bifeld, E.; Torrado, J.J.; Olías-Molero, A.I.; Corral, M.J.; Santarem, N.; Baptista, C.; Severi, L.; et al. Discovery of a benzothiophene-flavonol halting miltefosine and antimonial drug resistance in Leishmania parasites through the application of medicinal chemistry, screening and genomics. *Eur. J. Med. Chem.* **2019**, *183*, 111676. [[CrossRef](#)]
22. Kishore, N.R.; Ashok, D.; Sarasija, M.; Murthy, N.Y.S. One-pot synthesis of spirochromanone-based 3-hydroxy-4*H*-chromen-4-ones by a modified Algar–Flynn–Oyamada reaction and evaluation of their antimicrobial activity. *Chem. Heterocycl. Compd.* **2017**, *53*, 1187–1191. [[CrossRef](#)]
23. Ashok, D.; Kifah, M.A.; Lakshmi, B.V.; Sarasija, M.; Adam, S. Microwave-assisted one-pot synthesis of some new flavonols by modified Algar–Flynn–Oyamada reaction and their antimicrobial activity. *Chem. Heterocycl. Compd.* **2016**, *52*, 172–176. [[CrossRef](#)]
24. Lee, J.; Park, T.; Jeong, S.; Kim, K.-H.; Hong, C. 3-Hydroxychromones as cyclin-dependent kinase inhibitors: Synthesis and biological evaluation. *Bioorg. Med. Chem. Lett.* **2007**, *17*, 1284–1287. [[CrossRef](#)] [[PubMed](#)]
25. Joshi, H.C.; Antonov, L. Excited-State Intramolecular Proton Transfer: A Short Introductory Review. *Molecules* **2021**, *26*, 1475. [[CrossRef](#)]
26. Ameer-Beg, S.; Ormson, S.M.; Brown, R.G.; Matousek, P.; Towrie, M.; Nibbering, E.T.J.; Foggi, P.; Neuwahl, F.V.R. Ultrafast Measurements of Excited State Intramolecular Proton Transfer (ESIPT) in Room Temperature Solutions of 3-Hydroxyflavone and Derivatives. *J. Phys. Chem. A* **2001**, *105*, 3709–3718. [[CrossRef](#)]
27. Sarkar, M.; Ray, J.G.; Sengupta, P.K. Effect of reverse micelles on the intramolecular excited state proton transfer (ESPT) and dual luminescence behaviour of 3-hydroxyflavone. *Spectrochim. Acta A Mol. Biomol.* **1996**, *52*, 275–278. [[CrossRef](#)]
28. Zhao, X.; Li, X.; Liang, S.; Dong, X.; Zhang, Z. 3-Hydroxyflavone derivatives: Promising scaffolds for fluorescent imaging in cells. *RSC Adv.* **2021**, *11*, 28851. [[CrossRef](#)]
29. Butun, B.; Topcu, G.; Ozturk, T. Recent Advances on 3-Hydroxyflavone Derivatives: Structures and Properties. *Mini Rev. Med. Chem.* **2018**, *18*, 98–103. [[CrossRef](#)]
30. Russo, M.; Orel, V.; Takko, P.; Šranková, M.; Muchová, L.; Vitek, L.; Klán, P. Structure–Photoreactivity Relationship of 3-Hydroxyflavone-Based CO-Releasing Molecules. *J. Org. Chem.* **2022**, *87*, 4750–4763. [[CrossRef](#)]
31. Jiang, G.; Jin, Y.; Li, M.; Wang, H.; Xiong, M.; Zeng, W.; Yuan, H.; Liu, C.; Ren, Z.; Liu, C. Faster and More Specific: Excited-State Intramolecular Proton Transfer-Based Dyes for High-Fidelity Dynamic Imaging of Lipid Droplets within Cells and Tissues. *Anal. Chem.* **2020**, *92*, 10342–10349. [[CrossRef](#)] [[PubMed](#)]
32. Kamariza, M.; Keyser, S.G.L.; Utz, A.; Knapp, B.D.; Ealand, C.; Ahn, G.; Cambier, C.J.; Chen, T.; Kana, B.; Huang, K.C.; et al. Toward Point-of-Care Detection of Mycobacterium tuberculosis: A Brighter Solvatochromic Probe Detects Mycobacteria within Minutes. *JACS Au* **2021**, *1*, 1368–1379. [[CrossRef](#)] [[PubMed](#)]
33. Bernini, R.; Crisante, F.; Ginnasi, M.C. A Convenient and Safe O-Methylation of Flavonoids with Dimethyl Carbonate (DMC). *Molecules* **2011**, *16*, 1418–1425. [[CrossRef](#)] [[PubMed](#)]
34. Koirala, N.; Thuan, N.H.; Ghimire, G.P.; Thang, D.V.; Sohng, J.K. Methylation of flavonoids: Chemical structures, bioactivities, progress and perspectives for biotechnological production. *Enzym. Microb.* **2016**, *86*, 103–116. [[CrossRef](#)] [[PubMed](#)]

35. Liu, Y.; Fernie, A.R.; Tohge, T. Diversification of Chemical Structures of Methoxylated Flavonoids and Genes Encoding Flavonoid-O-Methyltransferases. *Plants* **2022**, *11*, 564. [[CrossRef](#)] [[PubMed](#)]
36. Ohtani, H.; Ikegawa, T.; Honda, Y.; Kohyama, N.; Morimoto, S.; Shoyama, Y.; Juichi, M.; Naito, M.; Tsuruo, T.; Sawada, T. Effects of various methoxyflavones on vincristine uptake and multidrug resistance to vincristine in P-gp-overexpressing K562/ADM cells. *Pharm. Res.* **2007**, *24*, 1936–1943. [[CrossRef](#)]
37. Juvale, K.; Stefan, K.; Wiese, M. Synthesis and biological evaluation of flavones and benzoflavones as inhibitors of BCRP/ABCG. *Eur. J. Med. Chem.* **2013**, *67*, 115–126. [[CrossRef](#)]
38. Khan, D.; Parveen, I.; Shaily, S.S. Design, Synthesis and Characterization of Aurone Based  $\alpha,\beta$ -unsaturated Carbonyl-Amino Ligands and their Application in Microwave Assisted Suzuki, Heck and Buchwald Reactions. *Asian J. Org. Chem.* **2022**, *11*, e202100638. [[CrossRef](#)]
39. Khan, D.; Parveen, I. Chroman-4-one-Based Amino Bidentate Ligand: An Efficient Ligand for Suzuki-Miyaura and Mizoroki-Heck Coupling Reactions in Aqueous Medium. *Eur. J. Org. Chem.* **2021**, *35*, 4946–4957. [[CrossRef](#)]
40. Joo, Y.H.; Kim, J.K.; Kang, S.-H.; Noh, M.-S.; Ha, J.Y.; Choi, J.C.; Lim, K.M.; Lee, C.H.; Chung, S. 2,3-Diarylbenzopyran derivatives as a novel class of selective cyclooxygenase-2 inhibitors. *Bioorg. Med. Chem. Lett.* **2003**, *13*, 413–417. [[CrossRef](#)]
41. Prasanna, S.; Manivannan, E.; Chaturvedi, S.C. Quantitative structure–activity relationship analysis of a series of 2,3-diaryl benzopyran analogues as novel selective cyclooxygenase-2 inhibitors. *Bioorg. Med. Chem. Lett.* **2004**, *14*, 4005–4011. [[CrossRef](#)]
42. O'Brien, D.F.; Gates, J.W., Jr. Some Reactions of 3-Hydroxy-1-phenylpyrazole. *J. Org. Chem.* **1966**, *31*, 1538–1542. [[CrossRef](#)]
43. Milišūnaitė, V.; Arbačiauskienė, E.; Řezníčková, E.; Jorda, R.; Malínková, V.; Žukauskaitė, A.; Holzer, W.; Šačkus, A.; Kryštof, V. Synthesis and anti-mitotic activity of 2,4- or 2,6-disubstituted- and 2,4,6-trisubstituted-2H-pyrazolo[4,3-c]pyridines. *Eur. J. Med. Chem.* **2018**, *150*, 908–919. [[CrossRef](#)] [[PubMed](#)]
44. Urbonavičius, A.; Fortunato, G.; Ambrazaitytė, E.; Plytninkienė, E.; Bieliauskas, A.; Milišūnaitė, V.; Luisi, R.; Arbačiauskienė, E.; Krikštolaitytė, S.; Šačkus, A. Synthesis and Characterization of Novel Heterocyclic Chalcones from 1-Phenyl-1H-pyrazol-3-ol. *Molecules* **2022**, *27*, 3752. [[CrossRef](#)] [[PubMed](#)]
45. Shen, X.; Zhou, Q.; Xiong, W.; Pu, W.; Zhang, W.; Zhang, G.; Wang, C. Synthesis of 5-substituted flavonols via the Algar-Flynn-Oyamada (AFO) reaction: The mechanistic implication. *Tetrahedron* **2017**, *73*, 4822–4829. [[CrossRef](#)]
46. Bhattacharyya, S.; Hatua, K. Computational insight of the mechanism of Algar–Flynn–Oyamada (AFO) reaction. *RSC Adv.* **2014**, *4*, 18702–18709. [[CrossRef](#)]
47. Ferreira, D.; Brandt, E.V.; Volstedt, F.D.R.; Roux, D.G. Parameters regulating the  $\alpha$ - and  $\beta$ -cyclization of chalcones. *J. Chem. Soc. Perkin Trans* **1975**, *1*, 1437–1446. [[CrossRef](#)]
48. Pati, S.K.; Marks, T.J.; Ratner, M.A. Conformationally Tuned Large Two-Photon Absorption Cross Sections in Simple Molecular Chromophores. *J. Am. Chem. Soc.* **2001**, *123*, 7287–7291. [[CrossRef](#)]
49. Jutand, A.; Mosleh, A. Rate and Mechanism of Oxidative Addition of Aryl Triflates to Zerovalent Palladium Complexes. Evidence for the Formation of Cationic ( $\sigma$ -Aryl)palladium Complexes. *Organometallics* **1995**, *14*, 1810–1817. [[CrossRef](#)]
50. Kumar, A.; Rao, M.L.N. Pot-economic synthesis of diarylpyrazoles and pyrimidines involving Pd-catalyzed cross-coupling of 3-trifloxychromone and triarylboron. *J. Chem. Sci.* **2018**, *130*, 165. [[CrossRef](#)]
51. Dahlén, K.; Wallén, E.A.A.; Grøtli, M.; Luthman, K. Synthesis of 2,3,6,8-Tetrasubstituted Chromone Scaffolds. *J. Org. Chem.* **2006**, *71*, 6863–6871. [[CrossRef](#)] [[PubMed](#)]
52. Akrawi, D.A.; Patonay, T.; Kónya, K.; Langer, P. Chemoselective Suzuki–Miyaura Cross-Coupling Reactions of 6-Bromo-3-(trifluoromethylsulfonyloxy)flavone. *Synlett* **2013**, *24*, 860–864. [[CrossRef](#)]
53. Nuzillard, J.-M. Use of carbon-13 NMR to identify known natural products by querying a nuclear magnetic resonance database—An assessment. *Magn Reson Chem* **2023**, *1*–7. [[CrossRef](#)] [[PubMed](#)]
54. Dolbier, W.R. *Guide to Fluorine NMR for Organic Chemists*; John Wiley & Sons, Inc.: Hoboken, NJ, USA, 2016.
55. Arbačiauskienė, E.; Martynaitis, V.; Krikštolaitytė, S.; Holzer, W.; Šačkus, A. Synthesis of 3-substituted 1-phenyl-1H-pyrazole-4-carbaldehydes and the corresponding ethanones by Pd-catalysed cross-coupling reactions. *ARKIVOC* **2011**, *11*, 1–21. [[CrossRef](#)]
56. Solum, M.S.; Altmann, K.L.; Strohmeier, M.; Berges, D.A.; Zhang, Y.; Facelli, J.C.; Pugmire, R.J.; Grant, D.M.  $^{15}\text{N}$  Chemical Shift Principal Values in Nitrogen Heterocycles. *J. Am. Chem. Soc.* **1997**, *119*, 9804–9809. [[CrossRef](#)]
57. Williamson, R.T.; Buevich, A.V.; Martin, G.E.; Parella, T. LR-HSQMBC: A Sensitive NMR Technique To Probe Very Long-Range Heteronuclear Coupling Pathways. *J. Org. Chem.* **2014**, *79*, 3887–3894. [[CrossRef](#)]
58. Barczyński, P.; Szafran, M.; Ratajczak-Sitarz, M.; Nowaczyk, Ł.; Dega-Szafran, Z.; Katrusiak, A. Structure of 2,3-dicarboxy-1-methylpyridinium chloride studied by X-ray diffraction, DFT calculation, NMR, FTIR and Raman spectra. *J. Mol. Struct.* **2012**, *1018*, 21–27. [[CrossRef](#)]
59. Iwatsuki, S.; Kanamitsu, Y.; Ohara, H.; Kawahata, M.; Danjo, H.; Ishihara, K. Crystal Structure of a Methanesulfonate Salt of 4-(N-Methyl)pyridinium Boronic Acid. *X-ray Struct. Anal. Online* **2012**, *28*, 63–64. [[CrossRef](#)]
60. Macdonald, A.L.; James Trotter, J. Crystal and molecular structure of o-benzoquinone. *J. Chem. Soc. Perkin Trans.* **1973**, *2*, 476–480. [[CrossRef](#)]
61. Allinger, N.L.; Chen, K.-H.; Lii, J.-H.; Durkin, K.A. Alcohols, ethers, carbohydrates, and related compounds. I. The MM4 force field for simple compounds. *J. Comput. Chem.* **2003**, *24*, 1447–1472.
62. Li, P.; Su, W.; Lei, X.; Xiao, Q.; Huang, S. Synthesis, characterization and anticancer activity of a series of curcuminoids and their half-sandwich ruthenium(II) complexes. *Appl. Organomet. Chem.* **2017**, *31*, e3685. [[CrossRef](#)]

63. Milišūnaitė, V.; Arbačiauskienė, E.; Bieliauskas, A.; Vilkauskaitė, G.; Šačkus, A.; Holzer, W. Synthesis of pyrazolo[4',3':3,4]pyrido[1,2-*a*]benzimidazoles and related new ring systems by tandem cyclisation of *vic*-alkynylpyrazole-4-carbaldehydes with (het)aryl-1,2-diamines and investigation of their optical properties. *Tetrahedron* **2015**, *71*, 3385–3395. [[CrossRef](#)]
64. Arbačiauskienė, E.; Krikštolaitytė, S.; Mitrulevičienė, A.; Bieliauskas, A.; Martynaitis, V.; Bechmann, M.; Roller, A.; Šačkus, A.; Holzer, W. On the Tautomerism of N-Substituted Pyrazolones: 1,2-Dihydro-3*H*-pyrazol-3-ones versus 1*H*-Pyrazol-3-ols. *Molecules* **2018**, *23*, 129. [[CrossRef](#)]
65. Titi, A.; Messali, M.; Alqurashy, B.A.; Touzani, R.; Shiga, T.; Oshio, H.; Fettouhi, M.; Rajabi, M.; Almalki, F.A.; Hadda, T.B. Synthesis, characterization, X-ray crystal study and bioactivities of pyrazole derivatives: Identification of antitumor, antifungal and antibacterial pharmacophore sites. *J. Mol. Struct.* **2020**, *1205*, 127625. [[CrossRef](#)]
66. Sharma, S.; Brahmachari, G.; Kant, R.; Gupta, V.K. One-pot green synthesis of biologically relevant novel spiro[indolin-2-one-3,4'-pyrano[2,3-*c*]pyrazoles] and studies on their spectral and X-ray crystallographic behaviors. *Acta Crystallogr. B Struct. Sci. Cryst. Eng. Mater.* **2016**, *72*, 335–343. [[CrossRef](#)] [[PubMed](#)]
67. Shynkar, V.V.; Mély, Y.; Duportail, G.; Piémont, E.; Klymchenko, A.S.; Demchenko, A.P. Picosecond Time-Resolved Fluorescence Studies Are Consistent with Reversible Excited-State Intramolecular Proton Transfer in 4'-(Dialkylamino)-3-hydroxyflavones. *J. Phys. Chem. A* **2003**, *107*, 9522–9529. [[CrossRef](#)]
68. Spadafora, M.; Postupalenko, V.; Shvadchak, V.; Klymchenko, A.; Mély, Y.; Burger, A.; Benhida, R. Efficient synthesis of ratiometric fluorescent nucleosides featuring 3-hydroxychromone nucleobases. *Tetrahedron* **2009**, *65*, 7809–7816. [[CrossRef](#)]
69. Klymchenko, A.S.; Ozturk, T.; Pivovarenko, V.G.; Demchenko, A.P. A 3-hydroxychromone with dramatically improved fluorescence properties. *Tetrahedron Lett.* **2001**, *42*, 7967–7970. [[CrossRef](#)]
70. Klymchenko, A.S.; Kenfack, C.; Duportail, G.; Mély, Y. Effects of polar protic solvents on dual emissions of 3-hydroxychromones. *J. Chem. Sci.* **2007**, *119*, 83–89. [[CrossRef](#)]
71. Voicescu, M.; Ionescu, S.; Gatea, F. Effect of pH on the fluorescence characteristics of some flavones probes. *Spectrochim. Acta A Mol. Biomol. Spectrosc.* **2014**, *123*, 303–308. [[CrossRef](#)]
72. Klymchenko, A.S.; Pivovarenko, V.G.; Ozturk, T.; Demchenko, A.P. Modulation of the solvent-dependent dual emission in 3-hydroxychromones by substituents. *New J. Chem.* **2003**, *27*, 1336–1343. [[CrossRef](#)]
73. Klymchenko, A.S.; Demchenko, A.P. Multiparametric probing of intermolecular interactions with fluorescent dye exhibiting excited state intramolecular proton transfer. *Phys. Chem. Chem. Phys.* **2003**, *5*, 461–468. [[CrossRef](#)]
74. Zhao, X.; Liu, Y.; Zhou, L.; Li, Y.; Chen, M. Time-dependent density functional theory study on excited state intramolecular proton transfer of 3-hydroxy-2-(pyridin-2-yl)-4*H*-chromen-4-one. *J. Lumin.* **2010**, *130*, 1431–1436. [[CrossRef](#)]
75. Chen, L.; Fu, P.-Y.; Wang, H.-P.; Pan, M. Excited-State Intramolecular Proton Transfer (ESIPT) for Optical Sensing in Solid State. *Adv. Optical Mater.* **2021**, *9*, 2170097. [[CrossRef](#)]
76. Ormson, S.M.; Brown, R.G.; Voller, F.; Rettig, W. Switching between charge- and proton-transfer emission in the excited state of a substituted 3-hydroxyflavone. *J. Photochem. Photobiol. A Chem.* **1994**, *81*, 65–72. [[CrossRef](#)]
77. Lebeau, B.; Innocenzi, P. Hybrid materials for optics and photonics. *Chem. Soc. Rev.* **2011**, *40*, 886–906. [[CrossRef](#)]
78. Mohammad-Pour, G.S.; de Coene, Y.; Wiratmo, M.; Maan, A.; Clays, K.; Masunov, A.E.; Crawford, K.E. Modular synthesis of zwitterionic, xanthene bridged, low twist angle chromophores with high hyperpolarizability. *Mater. Adv.* **2022**, *3*, 7520–7530. [[CrossRef](#)]
79. Andreu, R.; Carrasquer, L.; Santiago Franco, C.; Garín, J.; Orduna, J.; de Baroja, N.M.; Alicante, R.; Villacampa, B.; Allain, M. 4*H*-Pyran-4-ylidenes: Strong Proaromatic Donors for Organic Nonlinear Optical Chromophores. *J. Org. Chem.* **2009**, *74*, 6647–6657. [[CrossRef](#)]
80. Dolomanov, O.V.; Bourhis, L.J.; Gildea, R.J.; Howard, J.A.K.; Puschmann, H. A Complete Structure Solution, Refinement and Analysis Program. *J. Appl. Cryst.* **2009**, *42*, 339–341. [[CrossRef](#)]
81. Sheldrick, G.M. SHELXT-Integrated Space-Group and Crystal-Structure Determination. *Acta Cryst.* **2015**, *A71*, 3–8. [[CrossRef](#)]
82. Bourhis, L.J.; Dolomanov, O.V.; Gildea, R.J.; Howard, J.A.K.; Puschmann, H. The anatomy of a comprehensive constrained, restrained refinement program for the modern computing environment – Olex2 dissected. *Acta Cryst.* **2015**, *A71*, 59–75.

**Disclaimer/Publisher's Note:** The statements, opinions and data contained in all publications are solely those of the individual author(s) and contributor(s) and not of MDPI and/or the editor(s). MDPI and/or the editor(s) disclaim responsibility for any injury to people or property resulting from any ideas, methods, instructions or products referred to in the content.